AN ABSTRACT OF THE THESIS OF

Panupat Poocharoen for the degree of Master of Science in Electrical and Computer Engineering presented on March 15, 2005.

Title: LDPC-VBLAST for Wireless Communications

Abstract approved: Redacted for privacy

Mario E. Magaña

Recently, the demand for higher data rates of transmission has increased in many wireless communication applications. Using multi-transmit and multi-receive antennas has been shown to be a solution, since it can increase the channel capacity to accommodate higher transmission rates. Among the popular techniques developed to exploit the use of multiple antennas, VBLAST (Vertical Bell Laboratories Layered Space-Time) architecture can provide a very high spectral efficiency. However, in order to have better performance, an efficient error correction coding scheme with low complexity to implement is needed.

In this study, we applied the Low density parity-check (LDPC) codes to the multi-transmit and multi receive antennas system, by combining Euclidean geometry LDPC codes with VBLAST system. Different code rates and different numbers of antennas are evaluated. By Monte-Carlo simulation, it is shown that the combination of both LDPC-VBLAST improves the bit error rate performance of the conventional one. Higher code rates improve further bit error rate performance while maintaining a high transmission data rate. LDPC-VBLAST can achieve nearly the lower bound performance of LDPC coding used with the multiple antennas optimum detector, maximum likelihood (ML) detector, when increasing the number of receive antennas. However, unlike ML detector, LDPC-VBLAST has lower complexity than ML detector when increasing the number of antennas. Thus, LDPC_VBLAST can be suitable for using in many wireless applications.

LDPC-VBLAST for Wireless Communications

by

Panupat Poocharoen

A THESIS

submitted to

Oregon State University

in partial fulfillment of
the requirements for the
degree of

Master of Science

Presented March 15, 2005

Commencement June 2005

Master of Science thesis of Panupat Poocharoen

presented on March 15, 2005.

APPROVED:

Redacted for privacy

Major Professor, Electrical and Computer Engineering

Redacted for privacy

Director of the School of Electrical Engineering and Computer Science

Redacted for privacy

Dean of the Graduate School

I understand that my thesis will become part of the permanent collection of Oregon State University libraries. My signature below authorizes release of my thesis to any reader upon request.

Redacted for privacy

Panupat Poocharoen, Author

ACKNOWLEDGEMENTS

I would like to praise the Lord for giving me knowledge and wisdom. My parents who have always been beside me and given me their support. I also would like to thank and express my sincere appreciation to Dr. Mario E. Magaña who always gave me his advice in my studies, research and life during the time I was a student at Oregon State University. I would like to also thank Liang Xian who also provided comments and suggestions in my research.

CONTRIBUTION OF AUTHORS

The ideas behind increasing channel capacity by using multiple antennas were provided by G. J. Foschini and M. J. Gans. They provided the motivation for the studies in this Thesis, in order to develop and improve their methods by applying low density parity check codes. The generation of low density parity check codes using finite geometry approach and their decoding algorithm were drawn from the results obtained by Y. Kou, S. Lin and M. P. C. Fossorier. The performance of the contributed work which combined both schemes is compared with the theory and characteristics of multiple antennas obtained by J. G. Proakis.

TABLE OF CONTENTS

TABLE OF CONTENTS (Continued)

LIST OF FIGURES

LIST OF FIGURES (Continued)

Figure Page

LIST OF FIGURES (Continued)

Figure Page

To my parents, sisters and my beloved.

LDPC-VBLAST FOR WIRELESS COMMUNICATIONS

1 INTRODUCTION

Wireless technologies currently play important roles in many applications, such as, high-speed internet access, video and CD-quality music services. Many techniques have been studied and developed in order to support those sophisticated and high data rate applications.

According to Shannon-Hartley law [1], the maximum transmission rate of a signal with average power P over an additive white Gaussian noise (AWGN) channel with bandwidth B and power spectral density $N_0/2$, is equal to the channel capacity given by

$$C = B\log_2\left(1+\frac{P}{N_0 B}\right) \text{ bits per second.} \quad (1)$$

Typically, from the above equation, in order to provide high data rate communication with an arbitrarily small probability of error, it is possible to accomplish it either by increasing the signal transmitted power or system bandwidth. However, in practice, both are restricted and not available to change as desired. Error control coding and transmission diversity techniques are used instead to overcome errors that occur due to the receiver noise and fading channels.

Error control coding reduces the error probability of transmitted data. Many error control coding schemes are used in wireless communications, for instance, convolutional codes and Turbo codes. Recently, many researches have contributed to improve performance of low-density parity check codes. Low-density parity check (LDPC) codes are error correcting codes created by Gallager in 1960s [2]. At that time, the codes did not receive much attention of its importance until their rediscovery by MacKay *et al* in 1996 [3] while working on his 'MN codes' (MN stands for MacKay and Neal). Mackay showed that using sparse matrices to create a parity check

matrix provides a "good" error correcting code. The codes performances have been shown to achieve very near the Shannon limit, similar to Turbo codes. Because of the poor minimum distance problem in Turbo codes, LDPC codes outperform at very low bit error rates (BER < 10^{-5}) [3], [4]. Moreover, various types of decoding algorithms, from low to high complexity, make LDPC codes good candidates for channel encoding applications. In fact, they have now been designed for using in designing satellite digital video broadcasting standard, 4G mobile phones, hard drives, Earth link communications, etc..

The capacity of information transmitted can be increased by the number of antennas [5], [6], [7]. Multiple transmit and multiple receive antennas create a multiple input and multiple output (MIMO) system. MIMO systems have the advantage that they can send multiple streams of information at the same time. This creates transmit diversity which helps overcome the fading effect of a multipath transmission medium. Multiple receive antennas are used to distinguish each stream out from the other. One of the architectures designed for multiple antennas is VBLAST (Vertical Bell Laboratories Layered Space-Time) [23]. It has been shown in the past few years that the architecture provides a significant advantage, especially in a rich scattering environment, by using the benefit from the multipath transmission.

By combining both low density parity check codes and the VBLAST system (shortly will be called as LDPC-VBLAST system), it is intended to create an alternative system that would have a superior performance when used in wireless communications. The contribution of this thesis is to evaluate and analyze the effectiveness the combination. The thesis is organized as follows:

Chapter 2 provides the theoretical background of LDPC codes and focus on structured LDPC codes using a Euclidean geometry approach. Algorithms for generating both the encoder and decoder are provided. Computer simulations of their performance in a communication system for some code rates over a Gaussian channel are provided.

Chapter 3 provides the theoretical details of VBLAST system. We explain the principles of multiple antennas and its benefits of the increasing channel capacity.

Flat Rayleigh fading channel is introduced as the model of multipath effect of the transmission medium. We also compare the performance of VBLAST system with conventional linear detector along with the optimum receiver, the maximum likelihood detector.

Chapter 4 explains the details of LDPC-VBLAST system. The computer simulation results of the communication system using the proposed scheme in flat Rayleigh fading channel are provided. We then analyze and discuss the LDPC-VBLAST bit error rate performance using different code rates and different numbers of transmit and receive antennas.

Chapter 5 describes the conclusion and future work.

2. THEORETICAL DETAILS OF LDPC CODES

2.1 Characteristics of low-density parity check codes

Low Density Parity Check Codes, commonly called LDPC codes, are linear block codes which have low density of "ones" in the parity check matrix relative to its size. Thus, a parity check matrix of the code is a sparse matrix. The term sparse is used when the normalized density of ones in a vector or matrix is less than 0.5. The vector is very sparse if the density of ones decreases toward zero when the vector length is increased [3]. The sparseness enables the decoding algorithms to be simple and the information rates can be close to the Shannon limit, when optimal decoding is implemented. LDPC codes have the following properties [2], [4]:

1. The number of "ones" in each row and column must be constant.
2. The number of "ones" that are common between any two rows or columns is small. Preferably one.
3. The number of "ones" in each row and column is small compared with the length of the code and number of rows in the parity check matrix.

The codes that satisfy the above conditions are called "Regular LDPC Codes". However, if the number of "ones" in each row and column is varied, the generated codes are called "Irregular LDPC Codes". Considering the performance of the code, Irregular LDPC codes can nearly achieve Shannon capacity at low signal-to-noise ratio than regular LDPC. However, irregular LDPC codes have error floors approximately no less than 10^{-9}, while regular LDPC code can provide error floor less than 10^{-10} [8].

In order to meet the above requirements, many studies proposed several generating methods, which can be found in, e.g., [2], [3], [4], [9], [10]. These methods create LDPC codes in 2 fashions; non-structured, and structured code. Non-structured LDPC codes are randomly generated by using a computer. One can create both regular and irregular LDPC codes. The drawback is the complexity of the encoder and the difficulties in determining its properties. Structured LDPC codes are generated by analytic methods, such as algebraic or geometric approaches. Their advantage is the

capability to be decoded with several methods with less complexity. Therefore, in this thesis, LDPC codes are generated via a geometric approach.

The geometric approach proposed by Yu Kuo, Shu Lin and Marc P.C. Fossorier, uses the property of lines and points in a finite geometry. Two finite geometries are proposed: Euclidean (EG-LDPC codes) and Projective geometries (PG-LDPC codes) over a finite field. Since both provide similar performance, Euclidean geometry over finite field is chosen. More details of the approach can be found in [4].

2.2 Basics of LDPC codes

2.2.1 Linear block code

As mention, LDPC codes are linear block codes. They contain all the properties of a linear block code. This means,

- All possible input messages of length k bits $\mathbf{u} = (u_0, u_1, u_2, ..., u_{k-1})$, have one-to-one correspondence with 2^k code words $\mathbf{c} = (c_0, c_1, c_2, ..., c_{n-1})$ of length n bits.
- The set of 2^k code words, called C, form a k-dimensional subspace of the over all n-tuples vector space. Since the codes are linear, the sum of any code words in C results in another valid code word. Therefore, a code word $\mathbf{c} = (c_0, c_1, c_2, ...c_{n-1})$ can be written as

$$\mathbf{c} = u_0\mathbf{g}_0 + u_1\mathbf{g}_1 +, u_2\mathbf{g}_2 + ... + u_{k-1}\mathbf{g}_{k-1}$$

or

$$\mathbf{c} = \mathbf{u} \cdot \mathbf{G} \tag{2}$$

where $\mathbf{G} = \begin{bmatrix} \mathbf{g}_0 \\ \mathbf{g}_1 \\ \mathbf{g}_2 \\ \vdots \\ \mathbf{g}_{k-1} \end{bmatrix}$ is called generator matrix of size $k \times n$

and $\mathbf{g}_0, \mathbf{g}_1, \mathbf{g}_2, ..., \mathbf{g}_{k-1}$ are linear independent code words in C.

2.2.2 Parity Check Matrix

According to the concept of vector spaces, C is a subspace of an n-dimensional vector space and **G** consists of linearly independent code words (or vectors) from the subspace C. There exists a null space of C such that code words (vectors) from this null space are orthogonal to code words from C. Thus, the inner product of both codes will be zero. A parity check matrix is a matrix which consists of vectors from the null space of C. Multiplication of **c** with the parity check matrix would result in

$$\begin{aligned} \mathbf{s} &= \mathbf{c} \cdot \mathbf{H}_{LDPC}^{T} \\ &= \mathbf{u} \cdot \mathbf{G} \cdot \mathbf{H}_{LDPC}^{T} \\ &= \mathbf{u} \cdot \mathbf{0} \\ &= \mathbf{0}, \end{aligned} \tag{3}$$

where the vector $\mathbf{s} = (s_0, s_1, s_2, ..., s_{J-1})$ is called the syndrome vector or check sum. $\mathbf{H}_{LDPC}$ is a parity check matrix with size $J \times n$, where J is the number of orthogonal vectors. Normally, linear block codes would have $J = n - k$. However, it is different in the case of EG-LDPC codes which will be explained later. (Subscript *LDPC* is used to distinguish the matrix from the channel matrix $\mathbf{H}$).

It can be seen that $\mathbf{c} \cdot \mathbf{H}_{LDPC}^{T} = \mathbf{0}$. Therefore, the syndrome will equal to 0 when there is no error. If any error occurs during transmission of a code word, a non valid code word may result and the syndrome would not be equal to zero. Therefore, the code is capable of detecting and correcting errors depending on the minimum distance of the code.

2.3 Euclidean Geometry LDPC codes

This LDPC codes are constructed by using the concept of points and lines in m-dimensional Euclidean geometry over the Galois field GF(2^s) [11].

2.3.1 Concept of points

If we consider each element in GF(2^s) $=\{0,1,\beta^1,...,\beta^{2^s-2}\}$ as a point p on a dimension of Euclidean geometry, there will be 2^s points on each dimension. Thus, for an m-dimensional Euclidean geometry over GF(2^s), denoted as EG(m,2^s), will have 2^{ms} points. Each point then can be represented in m-tuples form as $\mathbf{p}=(p_0,p_1,p_2,p_3,...,p_{m-1})$, $p_0,p_1,p_2,p_3,...,p_{m-1} \in$ GF(2^s). The origin point of the geometry EG(m,2^s) is all-zero m-tuples, $\mathbf{0}$ = (0, 0, …, 0).

2.3.2 Concept of lines

The combination of points in Euclidean geometry can create lines (or planes, but planes will not be used). A line is also called 1-flat. A collection of 2^s points create a line, for instance, line $\{B\,\mathbf{p}\}$ where $B \in$ GF(2^s) and $\mathbf{p}$ is any 2^{ms}-1 non-origin point is a collection of points $\{0\cdot\mathbf{p}, 1\cdot\mathbf{p}, \beta\cdot\mathbf{p}, \ldots, \beta^{2^s-2}\,\mathbf{p}\}$. This line passes through the origin at $B = 0$. If a line passes through point $\mathbf{p}_0$, it is written as $\{\mathbf{p}_0 + B\mathbf{p}\}$, where $\mathbf{p}_0$ and $\mathbf{p}$ are both linearly independent. The collection of these points is then $\{\mathbf{p}_0+0\cdot\mathbf{p},\ \mathbf{p}_0+1\cdot\mathbf{p},\ \mathbf{p}_0+\beta\,\mathbf{p},\ \ldots\ ,\mathbf{p}_0+\beta^{2^s-2}\,\mathbf{p}\}$.

Lines are called parallel to each other if there is no point common in both lines. For example, $\{B\,\mathbf{p}\}$ and $\{\mathbf{p}_0 + B\mathbf{p}\}$ have no common points. Thus, they are parallel. From the 2^{ms} points in the geometry,

$$\text{Number of lines that are parallel to each other} = \frac{2^{ms}}{2^s} = 2^{(m-1)s}. \qquad (4)$$

Lines intersect each other if there is a point common in both lines. For example, line $\{\mathbf{p}_0 + B\mathbf{p}'\}$ and $\{\mathbf{p}_0 + B\mathbf{p}''\}$ are common at point $\mathbf{p}_0$. Thus, both intersect each other. Next, consider a point on the geometry. There are 2^{ms}-1 other points to make a combination. Each combination needs another 2^s-1 points in combination with the intersect point for creating a line. Therefore,

$$\text{Numbers of lines that intersect at a point} = \frac{2^{ms}-1}{2^{s}-1}. \tag{5}$$

The total lines in the Euclidean geometry are the summation of each parallel line with the lines intersected with it, i.e.,

$$\text{Total number of lines} = 2^{(m-1)s}\frac{2^{ms}-1}{2^{s}-1}. \tag{6}$$

2.3.3 Relation between parity check matrix and Euclidean geometry

Using a parity check matrix to map the relationship between the lines and points used in each combination, we can create a low density matrix. However, the origin point $\mathbf{0}$ = (0, 0, …, 0) and lines that intersect the origin would not be counted, since it could not be decoded using a majority-logic decoding scheme.

Let the parity check matrix $\mathbf{H}_{LDPC}$ have size $J \times n$. The n columns represent non-origin points. The numbers of non-origin points are

$$n = 2^{ms}-1. \tag{7}$$

J rows represent lines which do not pass through the origin. The representation of each line is also called an incident vector. Since there are $2^{(m-1)s}-1$ lines parallel to every line that passes through the origin point, then,

$$J = (2^{(m-1)s}-1)\frac{2^{ms}-1}{2^{s}-1}. \tag{8}$$

By using '1' to represent the location of points in the line and '0' otherwise, a parity check matrix with low density of ones can be created. Figure 1 shows an example of mapping the parity check matrix.

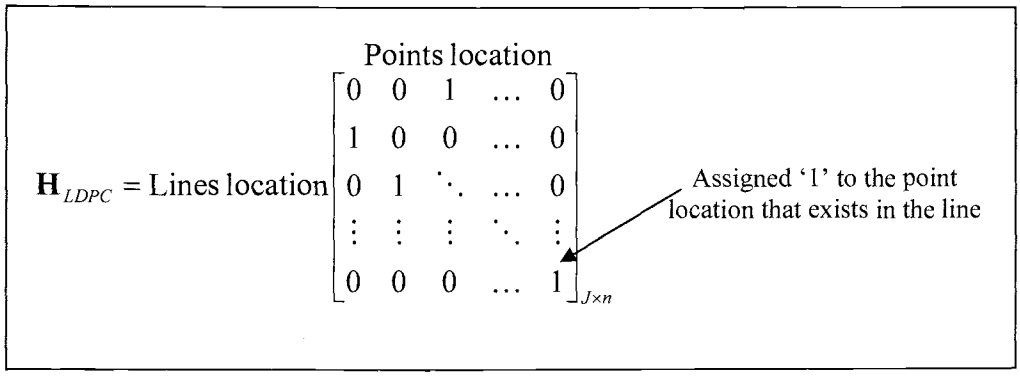

Figure 1: Demonstration of mapping parity check matrix with lines and points location

2.3.4 Finding lines and points from extended Galois field GF(2^{ms})

In order to calculate the location of points creating a line in m-dimensional Euclidean geometry over GF(2^s), the extension of Galois field GF(2^{ms}) is introduced. This can be explained as follows:

A Galois field GF (2^{ms}) has the primitive elements $\{0,1,\alpha^1,\alpha^2,\ldots,\alpha^{2^{ms}-2}\}$. GF($2^s$) is a subfield of GF ($2^{ms}$). Each of 2^{ms} primitive elements can also be expressed in polynomial form, i.e.,

$$\alpha^i = a_{i,0} + a_{i,1}\alpha^1 + a_{i,2}\alpha^2 + a_{i,j}\alpha^j + \ldots + a_{i,m-1}\alpha^{m-1}, \tag{9}$$

where $a_{i,j} \in GF(2^s), i \in \{\infty,0,1,2,\ldots,2^{ms}-2\}$ and $j \in \{0,1,2,\ldots,m-1\}$.

Thus, each primitive elements α^i of GF(2^{ms}) has one–to–one correspondence with a point $\mathbf{p}_i = (p_0, p_1, p_2, \ldots, p_{m-1})$ in EG(m,2^s), where $p_0, p_1, p_2, \ldots, p_{m-1} \in$ GF(2^s). The Galois field GF (2^{ms}) then is used for finding lines and their combination of points in an m-dimensional Euclidean geometry over GF(2^s). The procedure is outlined below.

1. Given a Euclidean geometry EG(m,2^s), find the primitive polynomial $\phi(X)$ in GF(2^{ms})

2. Letting β equal to any primitive element $\{0,1,\alpha^1,\alpha^2,\ldots,\alpha^{2^{ms}-2}\}$ of GF (2^{ms}), find the value of β that will create the finite field $\{0,1,\beta,\beta^2,\ldots,\beta^{2^s-2}\}$ for subfield GF(2^s).
3. Find all lines which intersect at $\mathbf{p}_0$. The collection of points for $\{\mathbf{p}_0 + B\mathbf{p}\}$ are

$$\{\mathbf{p}_0 + B\mathbf{p}\} = \{\alpha^0 + 0\cdot\mathbf{p},\quad \alpha^0 + 1\cdot\mathbf{p},\quad \alpha^0 + \beta\,\mathbf{p},\quad \ldots\quad ,\alpha^0 + \beta^{2^s-2}\,\mathbf{p}\}$$

Using $\mathbf{p} = \alpha^i$ for $i = 0,1,2,\ldots,2^{ms}-2$, there will be $\dfrac{2^{ms}-1}{2^s-1}$ lines. Only lines not passing through the origin are kept.

4. Repeat previous procedure to find lines intersecting at every point $\mathbf{p}_i$. The collection of points for $\{\mathbf{p}_i + B\mathbf{p}\}$ are

$$\{\mathbf{p}_i + B\mathbf{p}\} = \{\alpha^i + 0\cdot\mathbf{p},\quad \alpha^i + 1\cdot\mathbf{p},\quad \alpha^i + \beta\,\mathbf{p},\quad \ldots\quad ,\alpha^i + \beta^{2^s-2}\,\mathbf{p}\},$$

where $i = 0,1,2,\ldots,2^{ms}-2$. The parity check matrix then can be mapped from all lines and their combination of points.

2.3.5 Construction of parity check matrix of EG(2,2^2)

1. Since m=2 and s=2, GF(2^4) is used. The primitive polynomial $\phi(X) = 1 + X + X^4$ is chosen to create the primitive elements $\{0,1,\alpha^1,\alpha^2,\ldots,\alpha^{2^{ms}-2}\}$, such that $\phi(\alpha) = 1 + \alpha + \alpha^4 = 0$.
2. Given $\beta = \alpha^5$, then $\beta^\infty = 0$, $\beta^0 = 1$, $\beta^1 = \alpha^5$, $\beta^2 = \alpha^{10}$, β provides a finite field of $\{0,1,\beta,\beta^2\}$ for subfield $GF(2^2)$. Therefore, each primitive element of GF(2^{2*2}) can be represented as a point in 2-dimensional Euclidean geometry EG(2,2^2) written by polynomial expression as

Primitive Element	Polynomial
0	0
1	1
$\alpha^1 =$	α
$\alpha^2 =$	$\beta + \alpha$
$\alpha^3 =$	$\beta + \beta^2\alpha$
$\alpha^4 =$	$1 + \alpha$
$\alpha^5 =$	β
$\alpha^6 =$	$\beta\alpha$
$\alpha^7 =$	$\beta^2 + \beta\alpha$
$\alpha^8 =$	$\beta^2 + \alpha$
$\alpha^9 =$	$\beta + \beta\alpha$
$\alpha^{10} =$	β^2
$\alpha^{11} =$	$\beta^2\alpha$
$\alpha^{12} =$	$1 + \beta^2\alpha$
$\alpha^{13} =$	$1 + \beta\alpha$
$\alpha^{14} =$	$\beta^2 + \beta^2\alpha$

3. Finding the lines that intersect at $\mathbf{p}_0$. The collection of points for $\{\mathbf{p}_0 + B\mathbf{p}\}$ are

$$\{\mathbf{p}_0 + B\mathbf{p}\} = \{\alpha^0 + 0\cdot\mathbf{p},\ \alpha^0 + 1\cdot\mathbf{p},\ \alpha^0 + \beta\,\mathbf{p},\ \ldots\ ,\alpha^0 + \beta^{2^s-2}\,\mathbf{p}\}$$

For $\mathbf{p} = \alpha^0$,

$$\{\mathbf{p}_0 + B\alpha^0\} = \{\alpha^0 + 0\alpha^0, \alpha^0 + 1\alpha^0, \alpha^0 + \beta\alpha^0, \alpha^0 + \beta^2\alpha^0\}.$$

which

$$\alpha^0 + 0\alpha^0 = \alpha^0$$

$$\alpha^0 + 1\alpha^0 = 0$$

$$\begin{aligned}\alpha^0 + \beta\alpha^0 &= \alpha^0 + \alpha^5 \\ &= 1 + \alpha^4\alpha \\ &= 1 + (1+\alpha)\alpha \\ &= 1 + \alpha + \alpha^2 \\ &= \alpha^2(\alpha^2 + 1)\end{aligned}$$

$$
\begin{aligned}
&= \alpha^2(\alpha^4)^2 \\
&= \alpha^{10} \\
\alpha^0 + \beta^2\alpha^0 \quad &= \alpha^0 + \alpha^{10} \\
&= \alpha^5
\end{aligned}
$$

Thus, the collection of points for $\{\alpha^0 + B\alpha^0\} = \{\alpha^0, 0, \alpha^{10}, \alpha^5\}$. By continuing the process for $\mathbf{p} = \alpha^i$, $i = 0,1,2,...,2^{ms} - 2$, other lines are:

$$
\begin{aligned}
\{\mathbf{p}_0 + B\alpha^1\} \quad &= \{\alpha^0 + 0\alpha^1, \alpha^0 + 1\alpha^1, \alpha^0 + \beta\alpha^1, \alpha^0 + \beta^2\alpha^1\} \\
&= \{\alpha^0, \alpha^4, \alpha^{13}, \alpha^{12}\} \\
\{\mathbf{p}_0 + B\alpha^2\} \quad &= \{\alpha^0 + 0\alpha^2, \alpha^0 + 1\alpha^2, \alpha^0 + \beta\alpha^2, \alpha^0 + \beta^2\alpha^2\} \\
&= \{\alpha^0, \alpha^8, \alpha^9, \alpha^{11}\} \\
\{\mathbf{p}_0 + B\alpha^3\} \quad &= \{\alpha^0 + 0\alpha^3, \alpha^0 + 1\alpha^3, \alpha^0 + \beta\alpha^3, \alpha^0 + \beta^2\alpha^3\} \\
&= \{\alpha^0, \alpha^{14}, \alpha^2, \alpha^6\} \\
\{\mathbf{p}_0 + B\alpha^4\} \quad &= \{\alpha^0 + 0\alpha^4, \alpha^0 + 1\alpha^4, \alpha^0 + \beta\alpha^4, \alpha^0 + \beta^2\alpha^4\} \\
&= \{\alpha^0, \alpha^1, \alpha^{15}, \alpha^3\}
\end{aligned}
$$

Since line $\{\alpha^0, 0, \alpha^{10}, \alpha^5\}$ passes through the origin, therefore, it is not used.

4. Find lines intersecting at other point $\mathbf{p}_i$, for $i = 0,1,2,...,2^{ms} - 2$, using the same procedure. Represent each line as incident vectors $\mathbf{v} = (v_0, v_1, v_2, v_3, .., v_{2^{ms}-2})$. v_i=1 when the point α^i exists in the line. v_i=0 when point α^i is not. Then the parity check matrix of EG(2,2^2) is

$$\mathbf{H}_{LDPC} = \begin{array}{c} \\ v_1 \\ v_2 \\ v_3 \\ v_4 \\ v_5 \\ v_6 \\ v_7 \\ v_8 \\ v_9 \\ v_{10} \\ v_{11} \\ v_{12} \\ v_{13} \\ v_{14} \\ v_{15} \end{array} \begin{array}{c} \begin{array}{cccccccccccccc} \alpha^0 & \alpha^1 & \alpha^2 & \alpha^3 & \alpha^4 & \alpha^5 & \alpha^6 & \alpha^7 & \alpha^8 & \alpha^9 & \alpha^{10} & \alpha^{11} & \alpha^{12} & \alpha^{13} & \alpha^{14} \end{array} \\ \begin{bmatrix} 1 & 0 & 0 & 0 & 1 & 0 & 0 & 0 & 0 & 0 & 0 & 0 & 1 & 1 & 0 \\ 1 & 0 & 0 & 0 & 0 & 0 & 0 & 0 & 1 & 1 & 0 & 1 & 0 & 0 & 0 \\ 1 & 0 & 1 & 0 & 0 & 0 & 1 & 0 & 0 & 0 & 0 & 0 & 0 & 0 & 1 \\ 1 & 1 & 0 & 1 & 0 & 0 & 0 & 1 & 0 & 0 & 0 & 0 & 0 & 0 & 0 \\ 0 & 1 & 1 & 0 & 1 & 0 & 0 & 0 & 1 & 0 & 0 & 0 & 0 & 0 & 0 \\ 0 & 1 & 0 & 0 & 0 & 1 & 0 & 0 & 0 & 0 & 0 & 0 & 0 & 1 & 1 \\ 0 & 1 & 0 & 0 & 0 & 0 & 0 & 0 & 0 & 1 & 1 & 0 & 1 & 0 & 0 \\ 0 & 0 & 1 & 1 & 0 & 1 & 0 & 0 & 0 & 1 & 0 & 0 & 0 & 0 & 0 \\ 0 & 0 & 1 & 0 & 0 & 0 & 0 & 0 & 0 & 0 & 1 & 1 & 0 & 1 & 0 \\ 0 & 0 & 0 & 1 & 0 & 0 & 0 & 0 & 0 & 0 & 0 & 1 & 1 & 0 & 1 \\ 0 & 0 & 0 & 1 & 1 & 0 & 1 & 0 & 0 & 0 & 1 & 0 & 0 & 0 & 0 \\ 0 & 0 & 0 & 0 & 1 & 1 & 0 & 1 & 0 & 0 & 0 & 1 & 0 & 0 & 0 \\ 0 & 0 & 0 & 0 & 0 & 1 & 1 & 0 & 1 & 0 & 0 & 0 & 1 & 0 & 0 \\ 0 & 0 & 0 & 0 & 0 & 0 & 1 & 1 & 0 & 1 & 0 & 0 & 0 & 1 & 0 \\ 0 & 0 & 0 & 0 & 0 & 0 & 0 & 1 & 1 & 0 & 1 & 0 & 0 & 0 & 1 \end{bmatrix} \end{array} \tag{10}$$

2.4 Generator matrix of Euclidean Geometry LDPC codes

LDPC codes generated from lines in EG(m,2^s), or 1-flat, are known as (0,s)th-order EG codes. Euclidean geometry codes are a subclass of polynomial codes [12], [13], a class of cyclic code using polynomial approach. According to [11], the generator polynomial g(x) for (0,s)th-order EG code length 2^{ms}-1 is given by

$$\text{g(x)} = \text{LCM } \{\text{minimal polynomials of all } \alpha^h\},$$

where $\alpha^h \in \text{GF } (2^{ms})$ are the roots of g(x) which can be found by satisfying the condition

$$0 < \max_{0 \le l < s} W_{2^s}(h^{(l)}) \le (m-1)(2^s - 1), \tag{11}$$

$h^{(l)}$ is the remainder from $2^l h$ modulo 2^{ms}-1; with h any integer less than 2^{ms}-1 and l an integer between $0 \le l < s$.

$$2^l h = q(2^{ms} - 1) + h^{(l)} \tag{12}$$

$W_{2^s}(h^{(l)})$ is the 2s-weight of $h^{(l)}$ which is the summation of the coefficients of $h^{(l)}$ in radix form, that is,

$$W_{2^s}(h^{(l)}) = \sum_{i=0}^{m-1} \delta_i \,, \tag{13}$$

where

$$h^{(l)} = \delta_0 + \delta_1 2^s + \delta_2 2^{2s} + \ldots + \delta_{m-1} 2^{(m-1)s} \,. \tag{14}$$

After the generator polynomial g(x) are calculated, the input message length can be found. Having the highest degree of generator polynomial deg (g(x)) $= r-1$, the input message block length k bits are equal to

$$k = 2^{ms} - 1 - r \,. \tag{15}$$

2.5 Decoding methods for Euclidean Geometry LDPC codes

By having a structure from (0,s)th-order Euclidean geometry codes, it has some advantage over many non-structured LDPC codes for the decoding algorithm. Most non-structure forms are based on sum-product decoding algorithm (some literatures called "massage passing" method) [3],[15]. Even though it has been proved that the method is capable to have a BER performance very near the Shannon limit, the complexity is quite high [4].

For EG-LDPC codes, 6 methods were demonstrated in [4]. From low to high complexity, those methods are one-step majority-logic (MLG) decoding, Gallager's bit flipping (BF) decoding, weighted MLG decoding, weighted BF decoding, a posteriori probability (APP) decoding, and iterative decoding based on belief propagation (known as sum- product algorithm (SPA)).

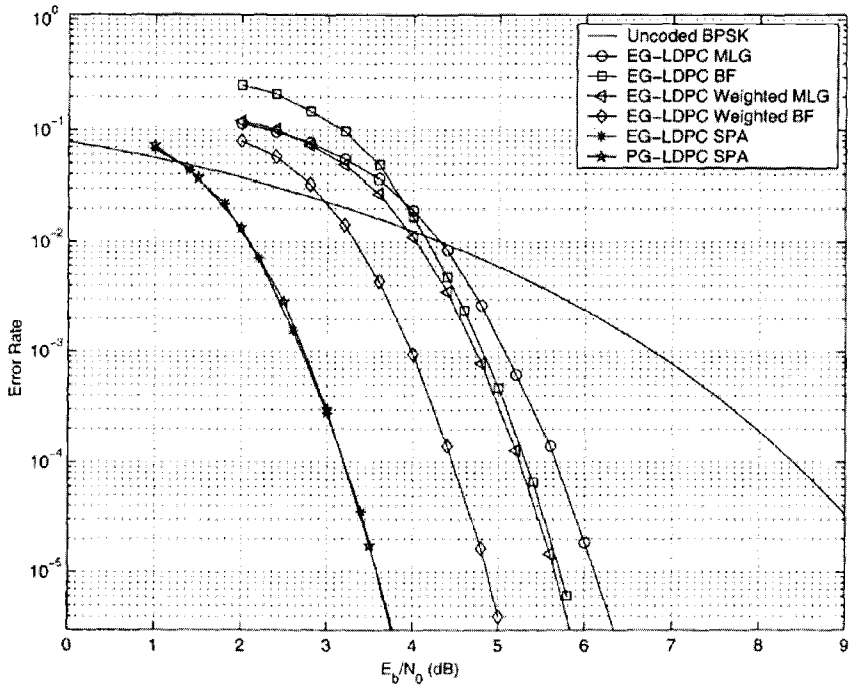

Figure 2: Bit-error probabilities of the type-I 2-D (255, 175) EG-LDPC code and (273, 191) PG-LDPC code based on different decoding algorithms. [4]

Figure 2 shows the difference in performance of each algorithm. The study shows that one-step majority-logic decoding is the simplest algorithm among the decoding methods, however, it has the worst error performance compared with the others. SPA provides the best error performance. Trading with a little of performance, much more simplicity, weighted BF decoding is chosen to be the decoding algorithm used in the LDPC-VBLAST system design instead of SPA algorithm. This also has been suggested in [4]. Due to its simplicity, it is attractive for using in high speed applications with a lower cost.

2.6 Weighted BF decoding algorithm

Weighted bit flipping decoding algorithm, hereafter called weighted BF, is a soft decision decoding method adapted from weighted-majority logic decoding [4],

[11], [12]. In fact, weighted bit flipping is an iterative version of weighted-majority logic decoding by correcting the bit with most "weight of errors" as the first priority.

Not all LDPC codes can be decoded by weighted bit flipping. According to [11], by having incident vectors which at any bit position i are all orthogonal to each other, EG-LDPC codes are one-step majority logic decodable. Therefore, weighted bit flipping decoding can be applied.

2.6.1 Orthogonality of vectors

If B incidence vectors $\mathbf{v}_j = (v_{j,0}, v_{j,1}, v_{j,2}, ..., v_{j,n-1})$, $0 \le j \le B$, are orthogonal at bit position $i = l$, where $0 \le l \le n-1$, then $v_{j,i=l}$ for all B vectors is equal to "1". The other $n-1$ positions, $v_{j,0}, v_{j,1}, \ldots, v_{j,l-1}, v_{j,l+1}, \ldots, v_{j,n-1}$, are either "1" or "0", but must have at most only one vector equal to "1". For instance, according to (10), the incidence vectors orthogonal at bit position $i = 5$ are

$$\mathbf{H}_{LDPC,\alpha^5} = \begin{array}{c} \\ v_1 \\ v_2 \\ v_3 \\ v_4 \end{array} \begin{array}{c} \begin{array}{cccccccccccccc} \alpha^0 & \alpha^1 & \alpha^2 & \alpha^3 & \alpha^4 & \alpha^5 & \alpha^6 & \alpha^7 & \alpha^8 & \alpha^9 & \alpha^{10} & \alpha^{11} & \alpha^{12} & \alpha^{13} & \alpha^{14} \end{array} \\ \begin{bmatrix} 0 & 1 & 0 & 0 & 0 & 1 & 0 & 0 & 0 & 0 & 0 & 0 & 0 & 1 & 1 \\ 0 & 0 & 1 & 1 & 0 & 1 & 0 & 0 & 0 & 1 & 0 & 0 & 0 & 0 & 0 \\ 0 & 0 & 0 & 0 & 1 & 1 & 0 & 1 & 0 & 0 & 0 & 1 & 0 & 0 & 0 \\ 0 & 0 & 0 & 0 & 0 & 1 & 1 & 0 & 1 & 0 & 0 & 0 & 1 & 0 & 0 \end{bmatrix} \end{array} .$$

Only at bit position i=5 all vectors are "1". At the other position, each has at most only one vector equal to "1". Thus, the number of orthogonal vectors numbers at each position in EG-LDPC matrix is $\frac{2^{ms}-1}{2^s-1} - 1$.

2.6.2 Weighted-majority logic decoding

Suppose the received signal is $\mathbf{y} = (y_0, y_1, y_2, ... y_{n-1})$ and its hard-decision equivalent binary sequence is $\mathbf{z} = (z_0, z_1, z_2, ... z_{n-1})$, then

$$\mathbf{z} = (\mathbf{y} + \mathbf{e}) \bmod 2, \qquad (16)$$

where $\mathbf{e} = (e_0, e_1, e_2, ...e_{n-1})$ is the error vector after performing the hard-decision operation. e_i=1 when an error at bit i occurs and 0 otherwise. Multiplying $\mathbf{z}$ with $\mathbf{H}_{LDPC}^T$, we get the check sum $\mathbf{s}$, i.e.,

$$\begin{aligned}\mathbf{s} &= \mathbf{z} \cdot \mathbf{H}_{LDPC}^T, \\ &= \mathbf{e} \cdot \mathbf{H}_{LDPC}^T, \\ &= \mathbf{e} \cdot \begin{bmatrix} \mathbf{v}_0 \\ \mathbf{v}_1 \\ \mathbf{v}_2 \\ \vdots \\ \mathbf{v}_J \end{bmatrix}^T .\end{aligned}$$

It can be seen that the check sum is not equal to 0. In order to correct the errors, the error pattern $\mathbf{e}$ must be found.

Consider bit position l. Among a total of J incidence vectors, there are $B = \frac{2^{ms}-1}{2^s-1} - 1$ incidence vectors orthogonal at l. The corresponding check sums, associate with (l), are $s_j^{(l)} = e_0 v_{j,0} + e_1 v_{j,1} + ... + e_{n-1} v_{j,n-1}$ modulo by 2, where $1 \le j \le B$. To find and correct the error pattern $\mathbf{e}$, instead of considering the majority value of check sums as one-step majority decoding, check sums are weighted by the magnitude of the received signal $\mathbf{y}$. Each check sum $s_j^{(l)}$ is first changed to a real value instead of binary {0, 1}, i.e., change "1" →1 and "0"→-1. Then $s_j^{(l)}$ are weighted differently using the minimum magnitude $|y_i|$ of bit positions that are checked by its incidence vector. That is,

$$\text{Weighted check sum } j \triangleq (2s_j - 1)\left|y_j\right|_{\min}, \tag{17}$$

where

$$\left|y_j\right|_{\min} = \min|y_i|, 0 \le i \le n-1 \text{ and } v_{j,i} = 1 \tag{18}$$

The summations of all B weighted check sums at bit position l are

$$E_l = \sum_{j=1}^{B} (2s_j^{(l)} - 1)\left|y_i\right|_{\min}^{(l)}. \tag{19}$$

By finding all E_l for $1 \le l \le n-1$, we will have error information for each bit. Using the criterion

$$E_l > 0, \text{ bit } l \text{ is wrong,} \tag{20}$$
$$E_l < 0, \text{ bit } l \text{ is correct.}$$

The larger the magnitude of E_l, the more likely it is. Therefore, error correcting is done by finding the highest positive value of E_l. Then, let the error pattern e_l=1 and flip the bit l by adding $\mathbf{z}$ with $\mathbf{e}$. Recalculate the check sums and continue procedure above until either all check sums are zero, or continue with the iterative procedure. A diagram depicting the above procedure is shown in figure 3.

2.6.3 Minimum distance and bit correcting capability

Based on the one-step majority-logic decoding criterion, the error correcting capability of the EG-LDPC code is equal to half of the number of incidence vectors orthogonal at any point. Therefore, EG-LDPC code has correcting capability equal to

$$t = \left\lfloor \frac{2^{ms} - 1}{2(2^s - 1)} - \frac{1}{2} \right\rfloor. \tag{21}$$

The minimum distance has a lower bound equal to

$$d_{\min} \ge \frac{2^{ms} - 1}{2^s - 1}. \tag{22}$$

For a special case that $m = 2$, equation (22) is the exact value of minimum distance [4].

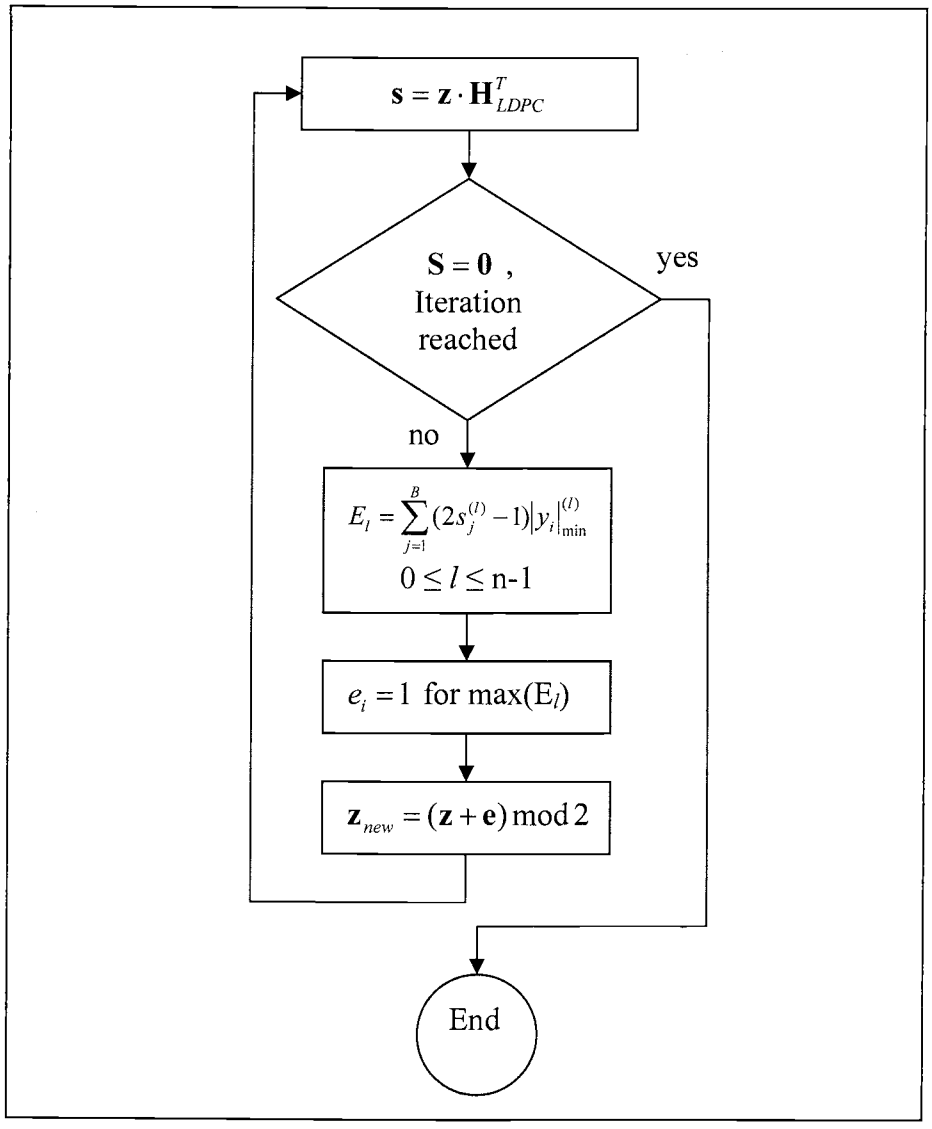

Figure 3: Diagram of weighted-BF decoding algorithm

2.7 Bit error rate performance for Euclidean Geometry codes

A typical communication system is shown in figure 4. We use this model to analyze its error correction performance.

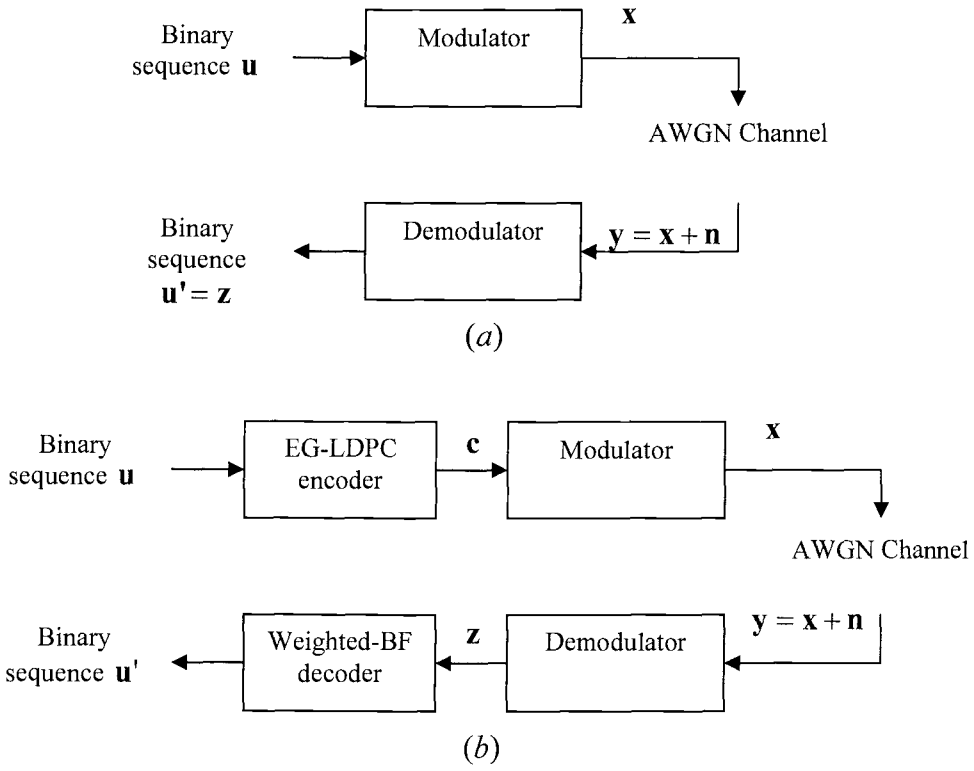

Figure 4: (a) Communication system model without using EG-LDPC codes
(b) Communication system model with EG-LDPC codes

System 1 in figure 4(a) is a communication model without applying channel encoding. The following assumptions are applied to the system:

1. $\mathbf{u} = (u_0, u_2, ..., u_{N-1})$, which is a sequence length N of binary data $i \in \{1,0\}$ with equally likely of occurrence, are transmitted.

2. Channel is considered to be ideal. That is, it has infinite bandwidth. Therefore, it has zero-intersymbol interference. Thus, pulse shaping and received filter are omitted.

3. Having all bits in $\mathbf{u}$ be statistically independent, they can be considered separately. Each bit is mapped into a rectangular pulse signal with amplitude $g(t) = \sqrt{E_b}(2i-1)$.

4. Signal $g(t)$ is then modulated with unit energy carrier using coherent binary phase shift keying (BPSK). The modulated signal is $x(t) = \sqrt{\frac{2E_b}{T_b}} \cos(2\pi f_c t + \pi(i-1))$ for $0 \le t \le T_b$, where T_b is the bit duration and $i = 1$ when bit sequence is "1", $i = 2$ when bit sequence is "0". f_c is the carrier frequency. To simplify the simulation, the transmitted signal is represented by its constellation value, i.e.,

$$x(t) = \sqrt{E_b}(2i-1) \qquad \text{for binary data } i = 1,0 \tag{23}$$

and the received signal after demodulator is

$$y(t) = x(t) + n(t) \tag{24}$$

where $y(t)$ is the received signal and $n(t)$ is the additive white Gaussian noise (AWGN) with zero mean, and variance $\sigma^2 = \frac{N_0}{2}$.

4. Hard decision is done by comparing with a threshold value

$$\begin{aligned} z(t) &= \text{"1"} \qquad \text{for } y(t) > 0 \\ z(t) &= \text{"0"} \qquad \text{for } y(t) < 0. \end{aligned} \tag{25}$$

System 2 in figure 4(b) is the communication model used with EG-LDPC code for error control coding. In addition to the assumptions applied to system 1, we also consider

5. Dividing the N bit binary sequence $\mathbf{u}$ into k bit blocks.

6. Each block is encoded into codeword $\mathbf{c} = (c_0, c_1, \ldots c_{n-1})$, block length $n = 2^{ms} - 1$, by EG-LDPC codes with EG(m,2^s).

7. Weighted-BF decoding algorithm is applied to decode the codeword.

Using Monte-Carlo simulation, the bit error rate performance of a BPSK system 1 (denoted as BPSK theory) and system 2 (denoted as BPSK using EG-LDPC codes) can be shown at different *energy per bit-to noise ratio* (E_b / N_0) as below figures.

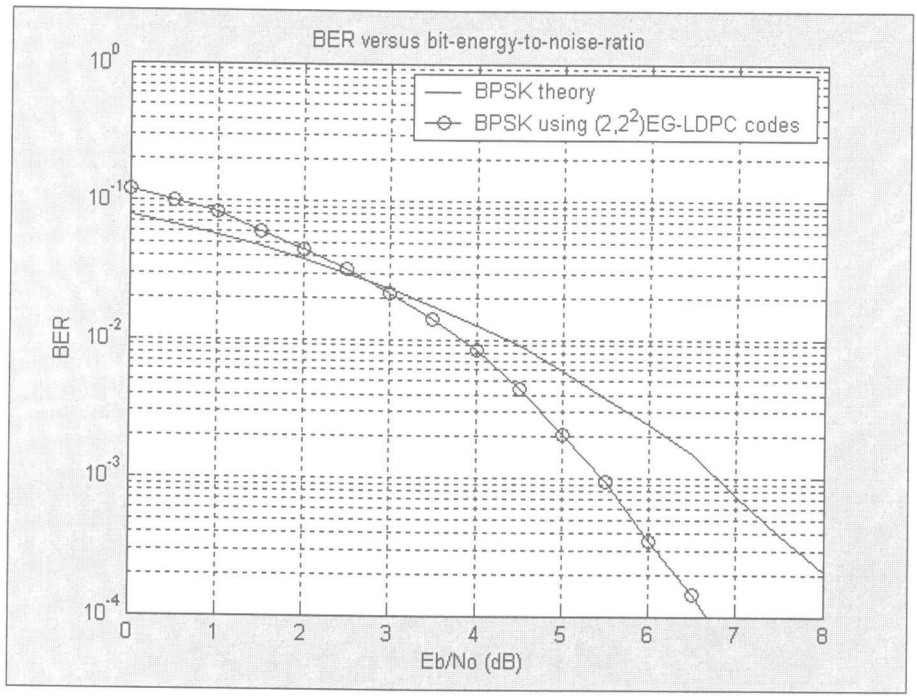

Figure 5: BER of BPSK system without error correction codes (theory)
Comparing with BPSK system with (15, 7) EG($2,2^2$)-LDPC code

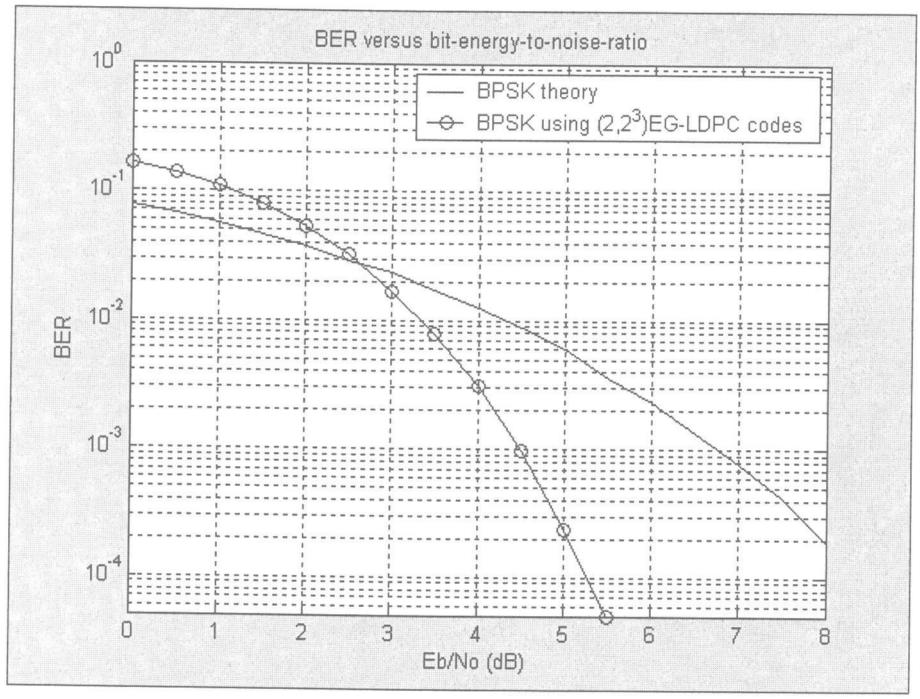

Figure 6: BER of BPSK system without error correction codes (theory) Comparing with BPSK system with (63,37) EG(2,2^3)-LDPC code

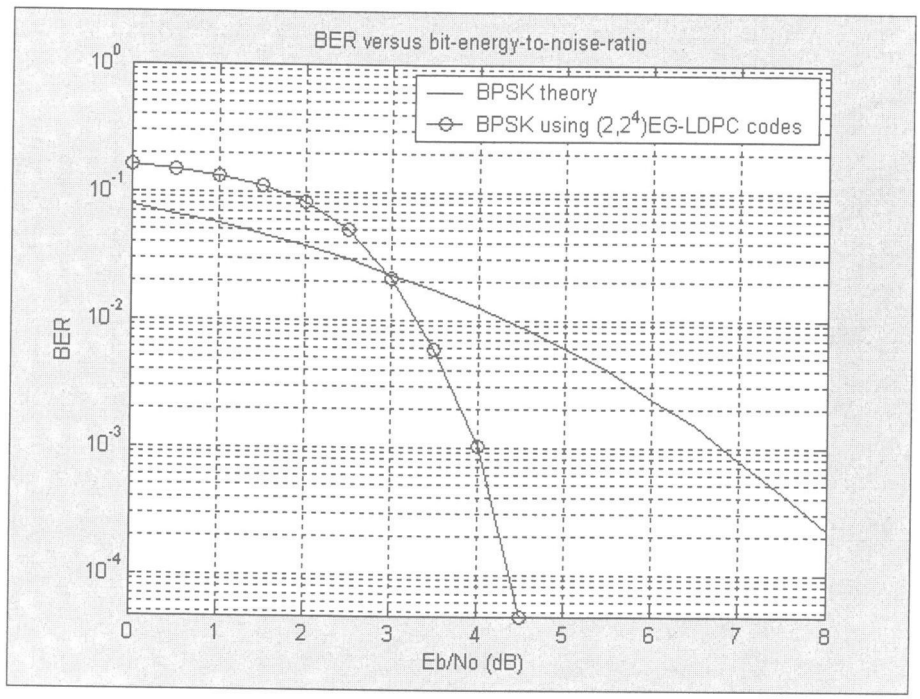

Figure 7: BER of BPSK system without error correction codes (theory) Comparing with BPSK system with (255, 175) EG(2,2^4)-LDPC code

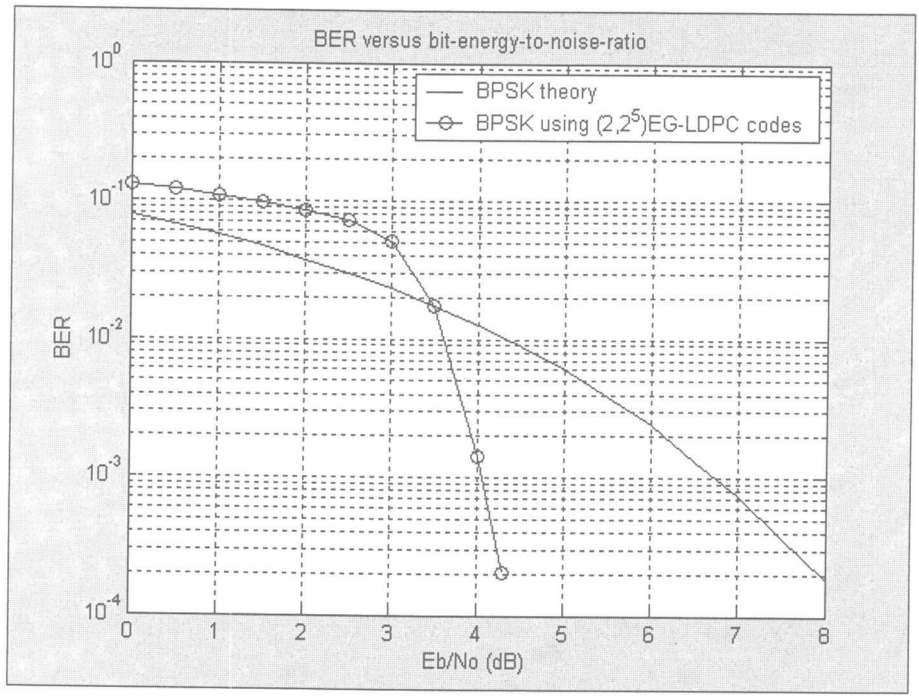

Figure 8: BER of BPSK system without error correction codes (theory) Comparing with BPSK system with (1023, 781) EG(2,2^5)-LDPC code

According the results shown in figures 5 to 8, the better bit error rate performance can be achieved by increasing the minimum distance of the code, since the minimum distance of the code characterizes the error correction capability. Increasing the minimum distance corresponds to increasing the code rate toward 1. In figures 5 to 8, we increase the minimum distance of the code by increasing the s value of the EG(m,2^s)-LDPC code. Even though comparing the result in figure 7 and 8, the system using the (255, 175) EG(2,2^4)-LDPC code seems to perform similar to the (1023, 781) EG(2,2^5)-LDPC code, the bit error rate of the (1023, 781) EG(2,2^5)-LDPC code decreases more rapidly when E_b / N_0 increases. Significant improvement can be seen clearly when comparing the system using the (255, 175) EG(2,2^4)-LDPC code and (15, 7) EG(2,2^2)-LDPC code in figure 6 and 5 , respectively.

2.8 Chapter summary

In this chapter, the characteristics of LDPC codes are explained. The theoretical details of generating Euclidean geometry LDPC (EG-LDPC) codes are provided. Weighted-BF is chosen to use for the decoding algorithm. Finally, the bit error rate performances of the code with some different code rates are shown by using Monte-Carlo simulation.

3. THEORETICAL DETAILS OF VBLAST SYSTEM

Many researchers developed new techniques to increase transmission rate near channel capacity and improve the performance of wireless systems using multi-element antennas. For instance, space-time block codes, space-time trellis codes, and VBLAST (Vertical Bell Laboratories Layered Space Time). In the case when there is no space constraint on the receiver side, namely, when the number of receiver antennas is equal to or greater than the number of transmitter antennas, VBLAST has an advantage because of its simplicity and high data transmission rate. Therefore, it is attractive for using in many future applications, e.g. Wireless Local Area Network, Digital/Audio Video Broadcasting (DAB/DVB-T) [7], etc..

3.1 Basic knowledge used for VBLAST system

3.1.1 Channel model and rich scattering environment

By using a different number of antennas at the transmitter and receiver sides, the communication system model over a channel would be modeled differently. For the VBLAST system, it can be modeled as Multiple Input Multiple Output system (MIMO), as shown in figure 9, where the number of receiver antennas N_r is equal to or greater than the number of transmitter antennas $N_t, (N_r \geq N_t)$. When N_t=1, VBLAST can also be viewed as Single Input Multiple Output (SIMO) or as a Single Input Single Output (SISO) system.

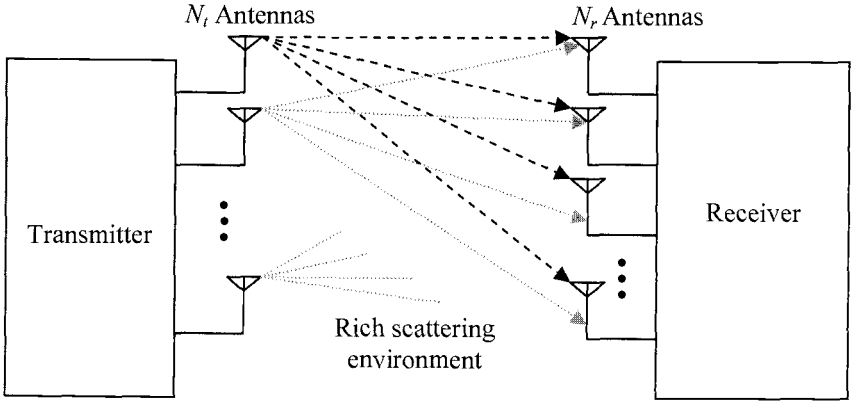

Figure 9: MIMO system model for multiple antennas used in VBLAST

Suppose the transmitted signals are expressed as vector, i.e., $\mathbf{x} = (x_0,...,x_{N_t-1})^T$, where $x_j, j \in \{0,1,...,N_t-1\}$, is transmitted by the j^{th} antenna. Let each transmitted signal propagate through an additive white Gaussian noise (AWGN) channel. All signals are received by each of the N_r receiver antennas. This can be modeled as

$$\mathbf{r} = \mathbf{H}\mathbf{x} + \mathbf{n}, \tag{26}$$

where $\mathbf{r} = (r_0, r_1,..., r_{N_r-1})^T$ is the received vector of signals from N_r antennas. $\mathbf{n} = (n_0, n_1,..., n_{N_r-1})^T$ is a noise vector with each element a complex white Gaussian noise random variable with zero mean and variance $\sigma^2 = N_0/2$. $\mathbf{H}$ is a channel matrix of size $N_r \times N_t$. with entries h_{ij}, $j \in \{0,1,...,N_t-1\}$ and $i \in \{0,1,...,N_r-1\}$. h_{ij} is equal to the channel coefficient due to transmitted signal x_j receiving at antenna i. In order to model the channel matrix $\mathbf{H}$, some assumptions are made.

1. Each antenna on both transmitter and receiver has sufficient spacing, at least half of wave length. The transmitted signal from each antenna then can be considered as having no mutual coupling. Therefore, each signal propagates through the channel independently.

2. The channel is considered to be a rich scattering environment, that is, multipath transmission occurs. If it is assumed that there is limited in mobility of the receiver, then the channel varies very slow compared to the signal transmission. In this case, the channel is assumed to be flat fading over the entire transmission signal frequency bandwidth, and having random magnitude with Rayleigh distribution.

3. The channel is also considered to be quasi-static, that is, the channel has constant magnitude and linear phase during a burst of signal but randomly change between each burst.

According to the above assumptions, each entry h_{ij} of $\mathbf{H}$ is an independent, identically distributed random variable (i.i.d.), which can be modeled as a summation between two quadrature random variables H_c and H_s, expressed by

$$h_{ij} = H_c + jH_s \tag{27}$$

where H_c and H_s are random variables with a Gaussian distribution $N(0,\sigma_h^2)$. Therefore, its envelope, $|h_{ij}|$ is a random variable

$$|h_{ij}| = \chi = \sqrt{H_c^2 + H_s^2} \tag{28}$$

with Rayleigh probability density function

$$f_\chi(x) = \frac{x}{\sigma_h^2} e^{-\left(\frac{x^2}{2\sigma_h^2}\right)} \quad , 0 \le x \le \infty \text{ and } \sigma_h > 0. \tag{29}$$

In addition, $|h_{ij}|^2 = H_c^2 + H_s^2$ also becomes a random variable with Chi-square probability density function (pdf) with two degrees of freedom, represented by symbol χ_2^2. The probability density function of χ_2^2 is

$$f_{\chi_2^2}(x) = \frac{1}{\sigma_h^2 2} e^{-\left(\frac{x}{2\sigma_h^2}\right)} \quad , 0 \le x \le \infty \text{ and } \sigma_h > 0. \tag{30}$$

There are many methods to generate the above fading channel for simulation, such as sum of sinusoidals model in Clarke and Gans fading model [15], Jakes' model [17 - 19], etc. However, if statistical performance is considered only, in computer simulation, it may also be simplified by using pseudo random generator to create H_c and H_s with $N(0,\sigma_h^2)$.

3.1.2 Channel capacity of MIMO channel

According to equation (26) and the aforementioned assumptions in section 3.1.1, let P be the total transmitted power and divided by N_t antennas equally. The channel capacity C_{MIMO} can be found by [6]

$$C_{MIMO} = \mathrm{E}\left\langle \log_2\left[\det\left(I_{N_r} + \frac{\rho}{N_t}\mathbf{H}\mathbf{H}^H \right)\right]\right\rangle \quad \text{bps/Hz.} \tag{31}$$

When the number of transmitted and received antennas each is equal to 1, the channel capacity is simply the same as Shannon-Hartley law in equation (1). This is true under the assumption that transmitter has no information of the channel but the channel is known to the receiver. ρ is the average signal power P to noise power ratio (SNR) at each branch of the receiving antenna. $\mathbf{H}^H$ is the complex conjugate transpose matrix of $\mathbf{H}$.

From the properties of the matrices, $\det\left(I_{N_r} + \frac{\rho}{N_t}\mathbf{H}\mathbf{H}^H\right) = \det\left(I_{N_t} + \frac{\rho}{N_t}\mathbf{H}^H\mathbf{H}\right)$, using $\mathbf{H}\mathbf{H}^H$ or $\mathbf{H}^H\mathbf{H}$ provides the same capacity. $\mathbf{H}$ is a $N_r \times N_t$ matrix with full rank, equal to $\min\{N_t, N_r\}$. By choosing $\mathbf{H}\mathbf{H}^H$ or $\mathbf{H}^H\mathbf{H}$ with smallest dimension $(\min\{N_t, N_r\} \times \min\{N_t, N_r\})$, we get a positive definite, square symmetric matrix. The $\min\{N_t, N_r\}$ provides the number of eigenvalues which are real and nonnegative. Thus, equation (31) can be written as

$$C_{MIMO} = \mathrm{E}\left\langle \sum_{i=1}^{\min(N_t,N_r)} \log_2\left[(1 + \frac{\rho}{N_t}\lambda_i) \right]\right\rangle, \tag{32}$$

which [6] shows that

$$C_{MIMO} = \int_0^\infty \log(1 + \frac{\rho}{N_t}\lambda) \sum_{k=0}^{\min(N_t,N_r)-1} \frac{k!}{(k+|N_t - N_r|)!} [L_k^{|N_t - N_r|}(\lambda)]^2 \lambda^{|N_t - N_r|} e^{-\lambda} d\lambda \tag{33}$$

Using the fact that logarithm is a concave function, the upper bound [7] of the capacity can be computed by using Jensen's inequality

$$C_{MIMO} \le \min(N_t, N_r) E\left\langle \log_2\left[1 + \frac{\rho}{\min(N_t, N_r)N_t} \sum_{i=1}^{\min(N_t, N_r)} \lambda_i\right]\right\rangle. \tag{34}$$

Again, applying Jensen's inequality, we get

$$C_{MIMO} \le \min(N_t, N_r) \log_2\left[1 + \frac{\rho}{\min(N_t, N_r)N_t} E\left\langle \sum_{i=1}^{\min(N_t, N_r)} \lambda_i \right\rangle\right]. \tag{35}$$

Since $E\left\langle \sum_{i=1}^{\min(N_t, N_r)} \lambda_i \right\rangle = E\left\langle Tr(\mathbf{H}^{\mathrm{H}}\mathbf{H})\right\rangle = \sum_{j=0}^{N_t-1}\sum_{i=0}^{N_r-1} E\left\langle |h_{ij}|^2 \right\rangle$, finally the upper bound is

$$C_{MIMO} \le \min(N_t, N_r) \log_2\left[1 + \frac{\rho}{\min(N_t, N_r)N_t} \sum_{j=0}^{N_t-1}\sum_{i=0}^{N_r-1} E\left\langle |h_{ij}|^2 \right\rangle\right]. \tag{36}$$

For analysis purposes, by making H_c and H_s equal to $N(0,1/\sqrt{2})$, we can normalize the power channel entries to 1, i.e., ($E\{|h_{ij}|^2\} = 1$). Hence, equation (34) becomes

$$C_{MIMO} \le \min(N_t, N_r) \log_2\left[1 + \frac{\rho \cdot N_r}{\min(N_t, N_r)}\right]. \tag{37}$$

Comparing with (1), it can be seen that the channel capacity depends on the signal-power-to noise ratio (SNR) and the $\min\{N_t, N_r\}$. When $N_t = N_r = n$, it can be seen that the channel capacity increases approximately n bps/Hz every 3dB (SNR) improvement.

3.2 VBLAST system

VBLAST is designed based on the characteristics of the channel known at receiver. The architecture of the VBLAST system for both transmitter and receiver are shown as a high level diagram in figure 10.

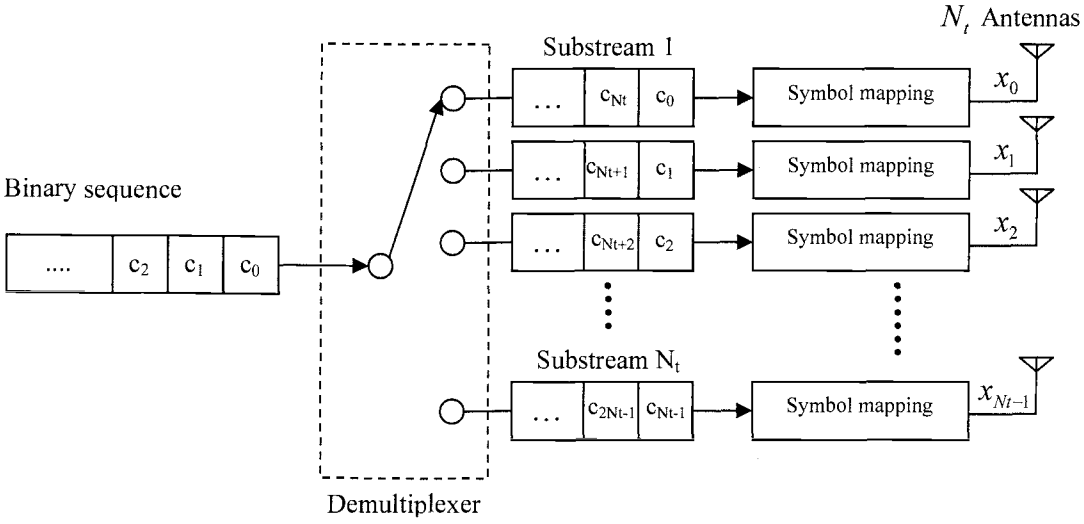

(a) Transmitter

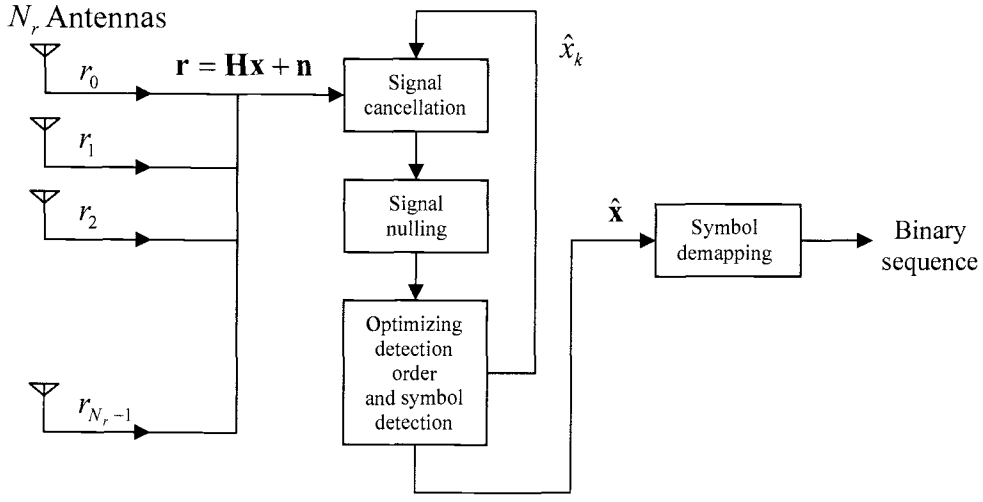

(b) Receiver

Figure 10: VBLAST architecture high level diagram

The transmitter of VBLAST is a multiplexer, which multiplexes binary sequences into N_T substreams. Each substream is then mapped into symbols, modulated, and then transmitted. The transmitted symbol vector is $\mathbf{x} = (x_0, x_1, ..., x_{N_t-1})^T$, and the received signal at the input of the demodulator is $\mathbf{r} = (r_0, r_1, ..., r_{N_r-1})^T$ as modeled in equation (26). Each received signal r at each branch of antennas is a signal combination of all transmitted symbols.

At the VBLAST receiver, three steps are taken iteratively: signal nulling, optimizing detection order and symbol detection, and signal cancellation. The purpose is to decorrelate the received signal and also cancel the interference from other signals. These steps can be viewed as ordered successive interference cancellation [22], or decision feedback equalizer [23].

Signal nulling can be done by multiplying the nulling matrix $G_{N_t \times N_r}$ by the received signal. The received signals are then decorrelated out from each other. This can be done by either using the zero forcing method (ZF) or the minimum mean square error method (MMSE). For the zero forcing method, the nulling matrix is

$$\mathbf{G} = \mathbf{H}^{+} = (\mathbf{H}^H \mathbf{H})^{-1} \mathbf{H}^H, \tag{38}$$

where $\mathbf{H}^{+}$ is the Moore-Penrose inverse [24] of $\mathbf{H}$. The decorrelated signal is then

$$\mathbf{y} = \mathbf{G}\mathbf{r} \tag{39}$$

$$= \mathbf{x} + \mathbf{H}^{+}\mathbf{n} \tag{40}$$

In the case of the minimum mean square error, the nulling matrix is

$$\mathbf{G} = (\mathbf{H}^H \mathbf{H} + \sigma^2 \mathbf{I}_{N_t})^{-1} \mathbf{H}^H. \tag{41}$$

where σ^2 is the noise variance. The decorrelated signal $\mathbf{y} = (y_0, y_1, ..., y_{N_t-1})^T$ is then

$$\mathbf{y} = (\mathbf{H}^{\mathrm{H}}\mathbf{H} + \sigma^2\mathbf{I}_{\mathrm{N_t}})^{-1}\mathbf{H}^{\mathrm{H}}\mathbf{H}\mathbf{x} + (\mathbf{H}^{\mathrm{H}}\mathbf{H} + \sigma^2\mathbf{I}_{N_t})^{-1}\mathbf{H}^{\mathrm{H}}\mathbf{n}\,. \tag{42}$$

When σ^2 is small compared to $\mathbf{H}^{\mathrm{H}}\mathbf{H}$, then it performs the same as the zero forcing in equation (40). When the $\mathbf{H}^{\mathrm{H}}\mathbf{H}$ is smaller than σ^2, the diagonal elements of equation (41) dominate the interference from other signals components.

Choosing the decorrelated signal with highest signal to noise ratio and cancel it out from each iterations, it has been shown to provide an optimal order of cancellation the interference. This can simply be considered by the minimum value of $\|\mathbf{G}\|_i^2$, the L2-norm for the i^{th} row of $\mathbf{G}$ [23]. Then the selected y_i is passed through the symbol detector which is a quantizer. This can be written as

$$\hat{x}_i = Q(y_i) \tag{43}$$

Next, $\hat{x}_i$ is cancelled out from $\mathbf{r}$ for the next iteration, which is

$$\mathbf{r}_{(next)} = \mathbf{r} - \mathbf{H}\hat{x}_i \tag{44}$$

The iterations continue to repeat from equations (38)-(44) until all $\hat{\mathbf{x}} = (\hat{x}_0, \hat{x}_1, ..., \hat{x}_{N_t-1})^T$ are extracted.

3.3 Bit error rate performance of VBLAST system

The following assumptions are made for simulating the bit error rate performance of VBLAST system.

1. Using the same model in of equation (26), binary phase-shift keyed signals $\mathbf{x} = (x_0, ..., x_{N_t-1})^T$ are transmitted simultaneously from N_t transmitting antennas with energy per symbol = E_s.

2. The channel is assumed to be quasi-static flat fading Rayleigh channel. Each channel matrix entry h_{ij} is modeled as an i.i.d complex random variable $h_{ij} = H_c + jH_s$. H_c and H_s are Gaussian random variables $N(0,1/\sqrt{2})$. Therefore, it has $E\{|h_{ij}|^2\} = 1$. Each received signal in $\mathbf{r} = (r_0, r_1, ..., r_{N_r-1})^T$ also contains AWGN with zero mean and variance $\sigma^2 = N_0/2$.

3. It is assumed that there is no mutual coupling between antennas.

4. Receiver side has the perfect knowledge of the channel. MMSE detector is selected for simulation.

5. Hereafter, we define the average signal-to-noise ratio per bit, $\bar{\gamma}_b$ at the receiver as the average signal energy per transmitted information bit to N_0. The definition provided is the same as in [29]. The total energy transmitted from all N_t antennas for symbol period T_s sec. are $E = N_t E_s$ where E_s is the symbol energy. By assuming the fading channel has $E\{|h_{ij}|^2\} = 1$, the total energy received from all N_r antennas is $N_r E$. The average received energy per information bit is then

$$E_b(\text{at receiver}) = \frac{N_r E}{r N_t C}, \tag{45}$$

where rN_tC is the total amount of information bit transmitted in period T_s. C is the number of coded bits per symbol and r is the code rate. Since in this chapter, the channel coding is not yet introduced to the system, r is equal to 1. and C is then equal to the information bit per symbol used. From equation (43), the average signal-to-noise ratio per bit $\bar{\gamma}_b$ at the receiver is

$$\bar{\gamma}_b = \left(\frac{E_b}{N_0}\right)_{receiver} = \frac{N_r E}{r N_t C N_0}. \tag{46}$$

Various cases of bit error rate versus average signal-to-noise ratio per bit $\bar{\gamma}_b$ at the receiver are simulated, with different number of transmitting and receiving antennas, using Monte Carlo simulation. The results are obtained as follow.

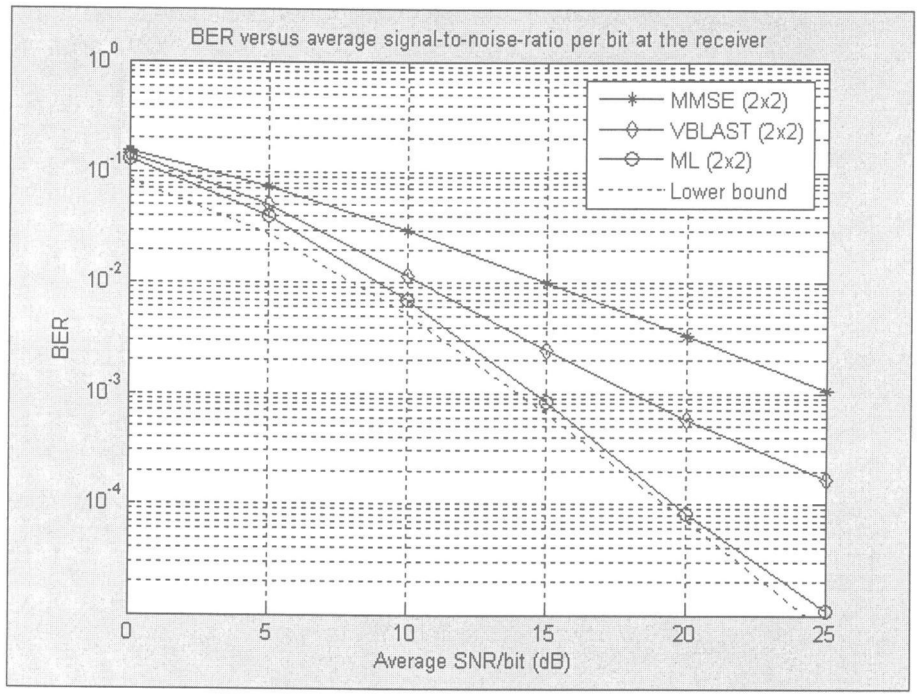

Figure 11: Bit-error rate performance of VBLAST system with $N_t = 2, N_r = 2$ compared with MMSE detector and Maximum likelihood (ML) detector with uncoded BPSK

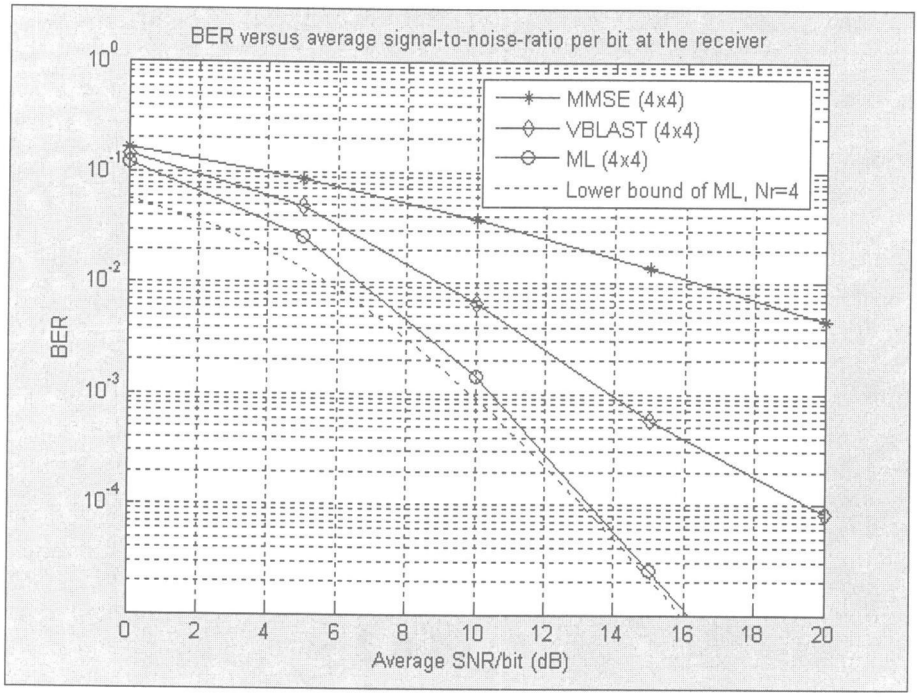

Figure 12: Bit-error rate performance of VBLAST system with $N_t = 4, N_r = 4$ compared with MMSE detector and Maximum likelihood (ML) detector with uncoded BPSK

Figures 11 and 12 show the bit error-rate performance of VBLAST system in a flat Rayleigh fading channel for $N_t = 2, N_r = 2$ and $N_t = 4, N_r = 4$ cases, respectively. MMSE linear detector without VBLAST and the maximum likelihood (ML) detector are chosen to compare with VBLAST in both cases. The maximum likelihood detector is the optimal detector for multi-transmit and multi-receive antennas. However, it suffers from high complexity which grows exponentially with the number of antennas and number of modulation symbols. Figure 11 shows that the bit error rate performance of the VBLAST is better than the MMSE linear detector, but inferior than ML detector.

In figure 12, we introduce the lower bound of ML detector in flat fading Rayleigh channel which can be calculated by [28]

$$P_e = \left[\tfrac{1}{2}(1-\mu)^{N_r}\right]\sum_{k=0}^{N_r-1}\binom{N_r-1+k}{k}\left[\tfrac{1}{2}(1+\mu)\right]^k, \qquad (47)$$

where

$$\mu = \sqrt{\frac{\bar{\gamma}_b}{N_r} \Big/ \left(1 + \frac{\bar{\gamma}_b}{N_r}\right)}. \tag{48}$$

Further details of this ML detector are now discussed. The result in equation (47) is also equal to the average error probability of maximum ratio combiner with N_r receiving antennas. Maximum ratio combiner is considered to be the ideal case for multi-transmit multi-receive antennas without signal interference. This means the system with multi-transmit and multi-receive antennas using ML detectors can achieve full diversity of N_r receiver antennas. Thus, the ML detector is the optimal detector. We then use this lower bound to compare with the performance of VBLAST system.

Increasing the number of receive antenna improves the bit error rate performance. It can be seen from the corresponding result in figure 13 and 14.

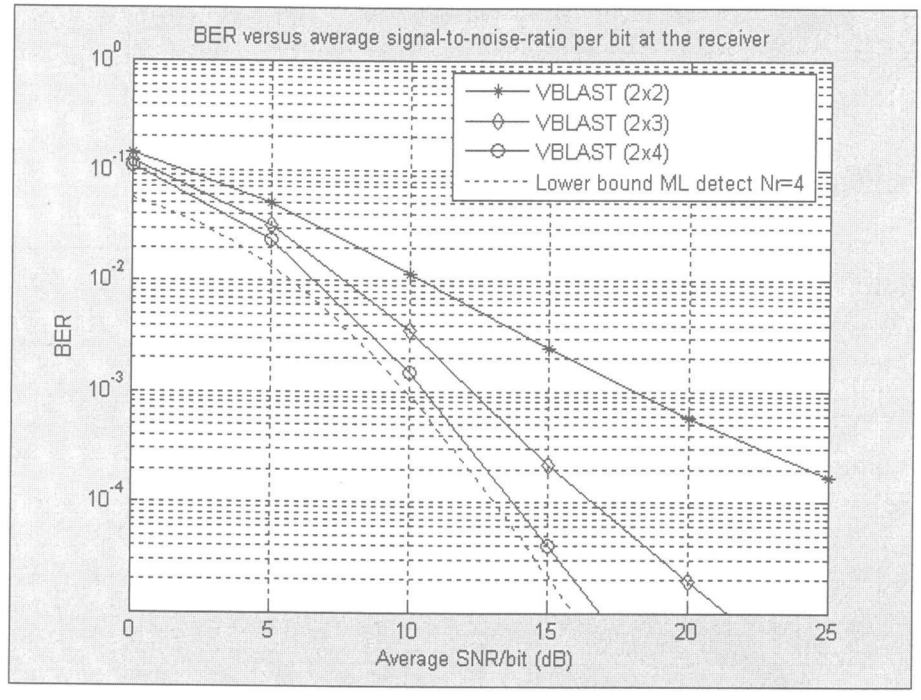

Figure 13: Bit-error rate performance of VBLAST system with $N_t = 2, N_r = 2$, $N_t = 2, N_r = 3$ and $N_t = 2, N_r = 4$ using BPSK

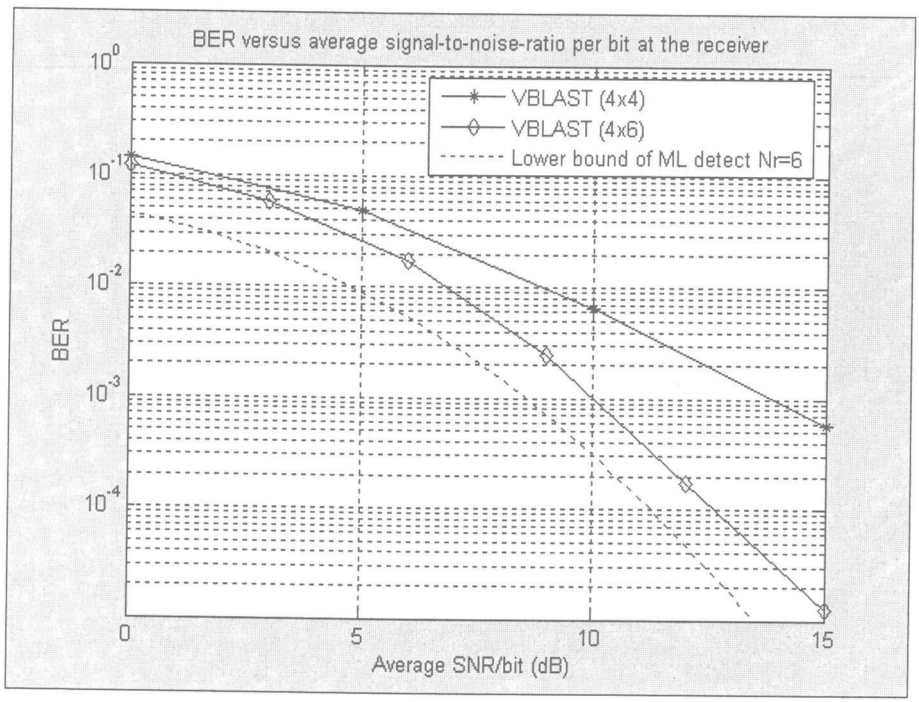

Figure 14: Bit-error rate performance of VBLAST system with $N_t = 4, N_r = 4$, and $N_t = 4, N_r = 6$ using BPSK

When the number of receive antennas increases, VBLAST system tends to perform better and nearly close to ML detector with N_t transmit and N_r receive antennas. Therefore, we may conclude that for the case that $N_r > N_t$ the lower bound of its performance tends to equal the ML detector.

3.4 Chapter summary

Multiple-transmit and multiple-receive antennas are introduced in this chapter. We have shown that the channel capacity can also be increased with more transmit and receive antennas. Therefore, higher data rate transmission is possible. Architecture of VBLAST is equal to the ordered successive interference cancellation. The performance of VBLAST can outperform the conventional linear detector. Even though it is inferior to the ML detector, it has less complexity. Thus VBLAST is shown to be attractive for using in high data rate transmission in wireless system.

4. LDPC-VBLAST SYSTEM AND SIMULATION RESULT

Here we propose a communication model for a multi-element antenna system which combines Euclidean geometry low density parity check code (LDPC) and VBLAST together, thereafter called LDPC-VBLAST system. The proposed system blocking diagram is shown in figure 15.

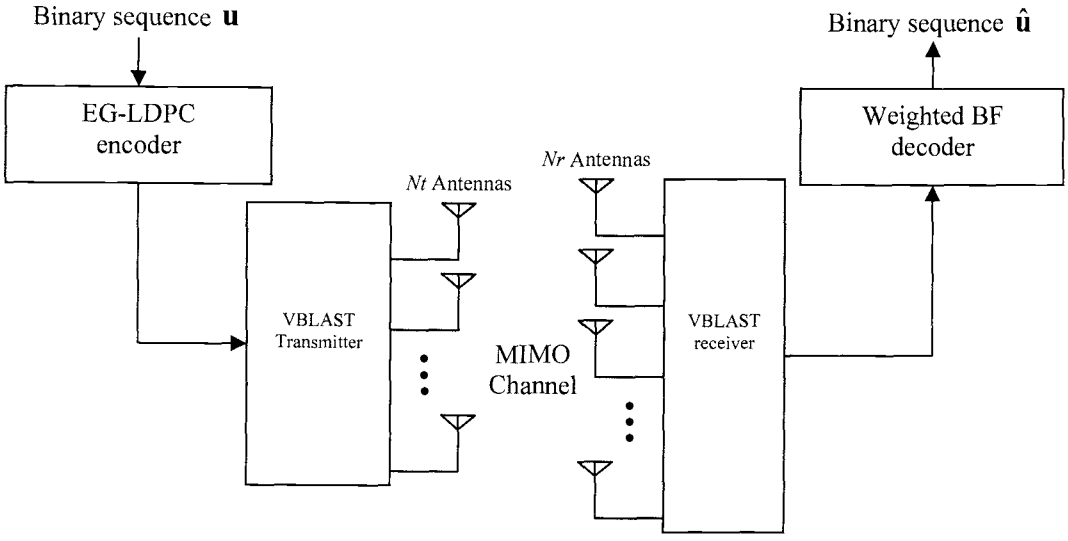

Figure 15: Model for LDPC-VBLAST system

Using the same conditions and assumptions as before, binary sequences with block size k bits are encoded into n-bit block codewords. The codewords are then demultiplexed into N_t substreams for N_t transmit antennas. Each substream is BPSK modulated and transmitted with energy per coded bit as $E_c = PT/N_t$, where P is the total transmission power and T is the symbol (bit) period.

The transmitted signals from all the antennas form a vector $\mathbf{x} = (x_0, x_1, ..., x_{N_t-1})^T$ which is transmitted to the receiver through a time dispersive channel plus additive white Gaussian noise (AWGN) with zero mean and variance $\sigma^2 = N_0/2$. The channel matrix $\mathbf{H}_{N_r \times N_t}$ is considered to be quasi-static, thus, flat fading. Each entry h_{ij} of $\mathbf{H}$,

$i \in \{0,1,...,N_r - 1\}$, and $j \in \{0,1,...,N_t - 1\}$ is an independent, identically distributed random variable (i.i.d.), whose random magnitude is Rayleigh distributed with $E\{|h_{ij}|^2\} = 1$.

At the receiver, the MMSE method is applied during the signal nulling step. Finally, weighted BF decoding is used to correct errors and decode the codeword. The decorrelated signal vector $\mathbf{y} = (y_0, y_1, ..., y_{N_t-1})^T$ is used as the weight for the estimated signal $\hat{\mathbf{x}} = (\hat{x}_0, \hat{x}_1, ..., \hat{x}_{N_t-1})^T$ in the decoding procedure.

Using this channel model and computer simulation, we proceed to evaluate the bit error rate performance of LDPC-VBLAST using different EG-LDPC code rates and the same number of transmit and receive antennas. We also simulate the bit error rate performance of LDPC VBLAST for MIMO systems using different numbers of antennas for the same EG-LDPC code rates. The simulation results using the Monte Carlo simulation method are shown in the following figures:

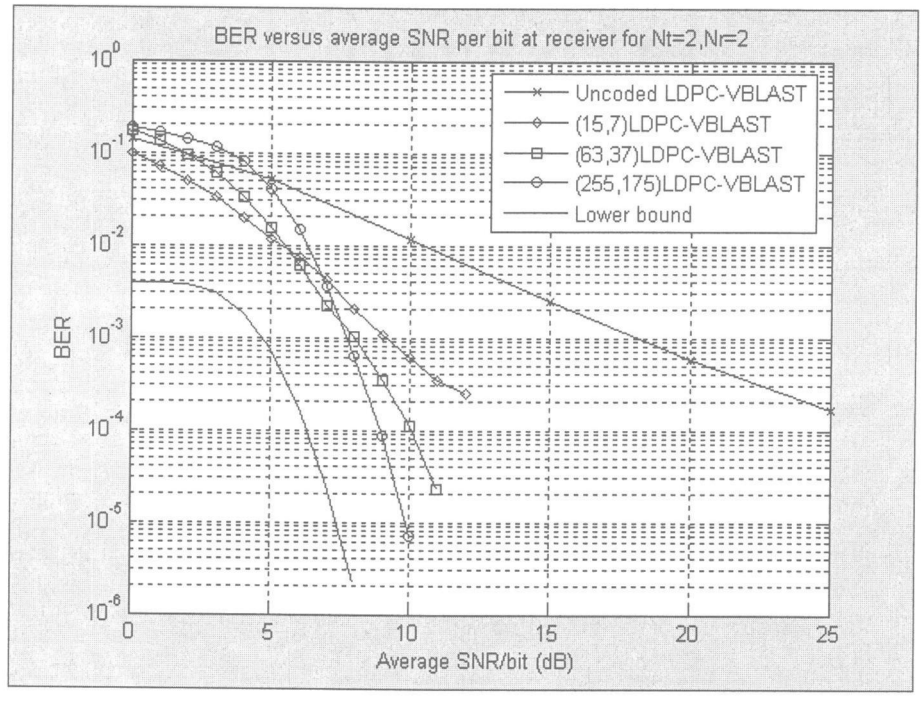

Figure 16: Bit-error probability of LDPC-VBLAST system ($N_t = 2, N_r = 2$) for different code rates along with uncoded VBLAST system using BPSK

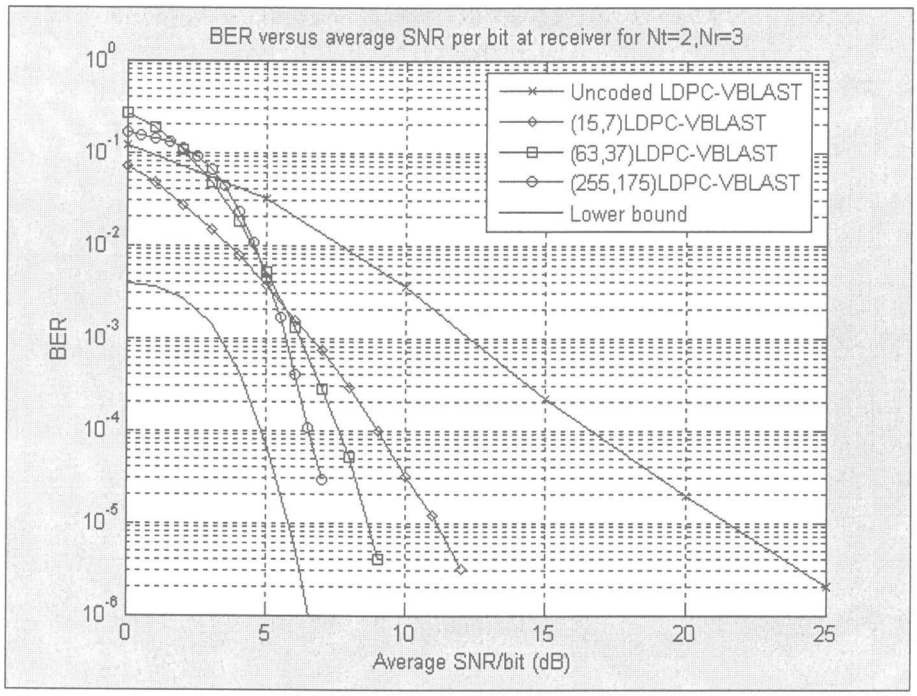

Figure 17: Bit-error probability of LDPC-VBLAST system ($N_t = 2, N_r = 3$) for different code rates along with uncoded VBLAST system using BPSK

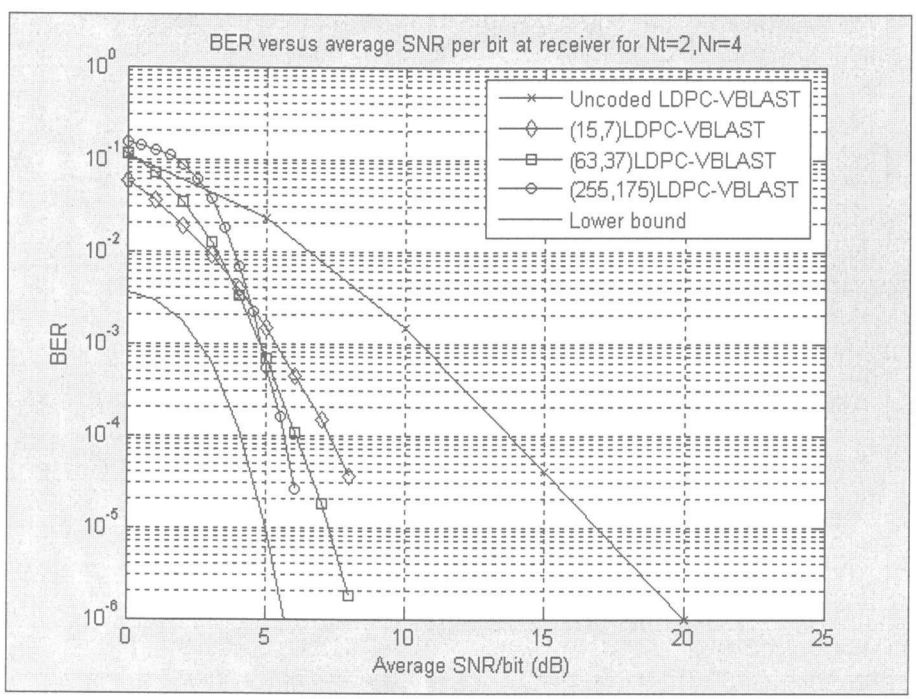

Figure 18: Bit-error probability of LDPC-VBLAST system ($N_t = 2, N_r = 4$) for different code rates along with uncoded VBLAST system using BPSK

Figures 16 to 18 show the performance results of LDPC VBLAST system with 2 transmit antennas and different numbers of receive antennas, i.e., 2, 3, and 4, respectively. It can be seen from these results that with the same number of transmit and receive antennas, LDPC-VBLAST can significantly improve the bit error rate performance compared with the uncoded VBLAST system. Moreover, the error correction ability can also be improved by changing parameters m and s of EG(2,2^s)-LDPC codes. In figures 16 to 18, we let m = 2 and vary the parameter s of EG(m,2^s)-LDPC code from 2, 3, and 4. This provides (15,7) EG(2,2^2)-LDPC code, (63,37) EG(2,2^3)-LDPC code, and (255,175) EG(2,2^4)-LDPC code, respectively. All figures show that the bit error rate of the VBLAST is improved.

As had been expected, using more receive antennas increases the receive diversity of the LDPC-VBLAST system which in turn improves the bit error rate performance. LDPC-VBLAST system with $N_t = 2, N_r = 4$ in figure 18 has a lower bit error rate comparing with LDPC-VBLAST system having $N_t = 2, N_r = 3$ and $N_t = 2$, $N_r = 2$, respectively.

Given the improvement of bit error rate performance of LDPC-VBLAST system over conventional VBLAST, we may then provide a lower bound of LDPC-VBLAST bit error probability using EG-LDPC code with weighted BF decoding algorithm as follows:

The probability of occurrence of i errors of a linear block code with word length n is

$$P(i,n) = \binom{n}{i} p^i (1-p)^{n-i} \tag{49}$$

where p is the bit error probability of VBLAST system. Since VBLAST is an iterative version of canceling interference, instead of providing the exact analytic form of its bit error probability, we may establish a lower bound for its performance. It was noted in the previous chapter that when receive antenna becomes larger than the number of transmit antenna, the bit error rate performance tends to move closer

towards ML detector performance with receive diversity order N_r. Therefore, it may be possible to assume that in the ideal case of VBLAST, the interference at each iterations (layer) is completely cancelled. Hence, VBLAST performs the same as ML detector. Therefore, we may set the lower bound for VBLAST performance using the lower bound of this optimum detector from equation (47) and we may let p equal to

$$p = P_e = \left[\tfrac{1}{2}(1-\mu)^{N_r}\right]\sum_{k=0}^{N_r-1}\binom{N_r-1+k}{k}\left[\tfrac{1}{2}(1+\mu)\right]^k.$$

According to equation (21), Weighted-BF algorithm has the capability to correct up to t errors, where

$$t = \left\lfloor \frac{2^{ms}-1}{2(2^s-1)} - \frac{1}{2} \right\rfloor.$$

If the code word has less than t errors, all the errors can be corrected. Some $t+1$ error patterns may also be able to be corrected. However, if the errors are equal or more than $t+2$, the errors can not be corrected. Thus, the lower bound of the error probability of the code word is

$$P_M \geq \sum_{i=t+2}^{n} P(i,n), \tag{50}$$

$$P_M \geq \sum_{i=t+2}^{n}\binom{n}{i} p^i (1-p)^{n-i}. \tag{51}$$

Since the code length n of EG-LDPC is equal to $2^{ms}-1$, we may provide an average bit error probability by dividing the error probability of the code word by n. Therefore, the lower bound of the average bit error probability for LDPC-VBLAST system using weighted-BF algorithm may be given as

$$BER \geq \frac{1}{2^{ms}-1}\sum_{i=t+2}^{2^{ms}-1}\binom{2^{ms}-1}{i}p^{i}(1-p)^{2^{ms}-1-i}. \qquad (52)$$

This bound is shown in figures 16, 17, and 18 which is the lower bound of (255,275) LDPC-VBLAST corresponding to its number of antennas using EG(2,2^4)-LDPC code. Figures 19 and 20 show the BER performance of the LDPC-VBLAST system using 4 receive and 4 transmit antennas. Both show the same trends as before.

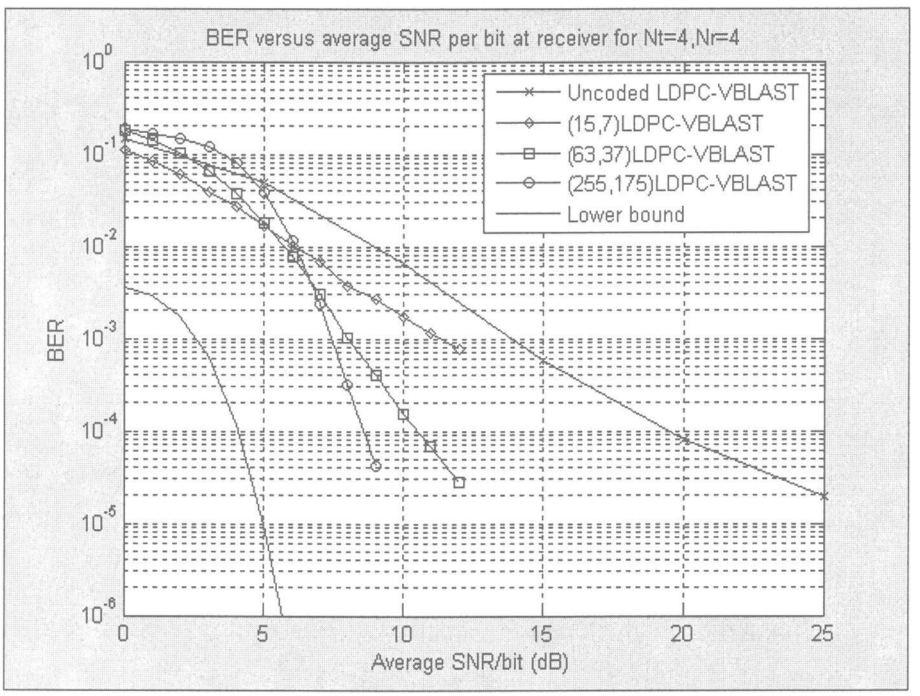

Figure 19: Bit-error probability of LDPC-VBLAST system ($N_t = 4, N_r = 4$) for different code rates along with uncoded VBLAST system using BPSK

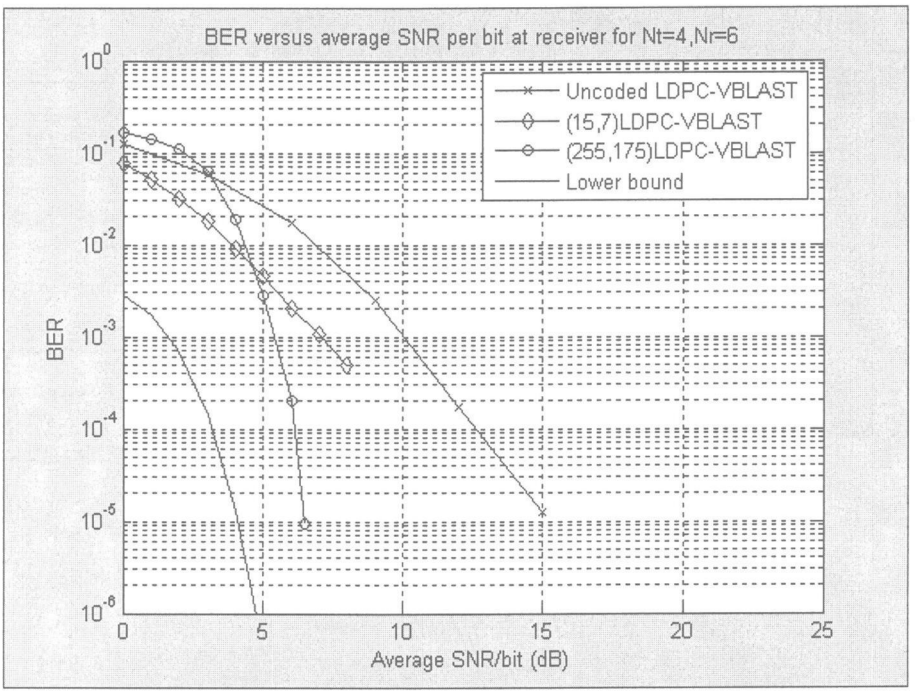

Figure 20: Bit-error probability of LDPC-VBLAST system ($N_t = 4, N_r = 6$) for different code rates along with uncoded VBLAST system using BPSK

It is noticeable when comparing LDPC-VBLAST system ($N_t = 4, N_r = 4$) with LDPC-VBLAST system ($N_t = 2, N_r = 2$) in figure 20 and 17 , respectively, that uncoded VBLAST provided better results for $N_t = 4, N_r = 4$ than $N_t = 2, N_r = 2$, but the performance at low code rate using (15,7) EG(2,2^2)-LDPC code or (63,37) EG(2,2^3)-LDPC code is quite similar or even worse. The reason may be that, at higher number of transmit and receive antennas if the wrong signal is detected at the initial layer of canceling the interference, it is more likely for the errors propagate to other layers in the detection process. Burst errors can happen more often with higher numbers of antennas. Therefore, low code rates which have a low error correction capability may not be able to correct all errors and also may even cause more propagation of errors. This also can be seen in the result of LDPC-VBLAST system ($N_t = 4, N_r = 6$) and LDPC-VBLAST system ($N_t = 2, N_r = 4$) in figures 21 and 19, respectively. However, it can be seen that in case of using (255,175) EG(2,2^4)-LDPC

code, the performance of $N_t = 4, N_r = 6$ becomes better than the case when $N_t = 2, N_r = 4$ antennas are used. Therefore, at higher numbers of transmit and receive antennas, higher code rate are required. Interleaving the coded data before transmission is expected to reduce the propagation errors in the decoder. However, further investigations must be conducted.

In short, several factors have an effect on the bit error rate performance of LDPC-VBLAST system. Some guidelines are suggested as below.

1. Selection of EG(m,2^s)-LDPC code. Since the values of the parameters m and s in the selected EG(m,2^s)-LDPC code determine the code length and the error correcting capability of the code. They must be considered carefully. One can be done by simply letting m=2 and change the value of s. If a fixed code rate is needed, puncturing (shortening) or extending LDPC code method can be completed. Further details can be found in [4].

2. Decoding algorithms. In our evaluation, we select Weighted-BF decoding algorithm. However, other decoding schemes may provide better performance. Simplicity of implementation at a lower cost may provide good enough performance.

3. Information transmission rate. If a higher transmission rate of information is needed, different modulation schemes, and a different number of transmit antennas may be needed. Also, in order to maintain the same bit error rate performance, a different code rate of LDPC code may need to be implemented.

It is noted that the simulations assume that each transmit and each receive antenna is separated from the other antennas far enough so that there is no correlation between the signals. In practice, this may not be the case when space is limited. It is shown in [31] that correlation between antennas degrades capacity of the channel. However, multiple antennas still provide better performance than single antenna system and can be used in many applications [5]

5. CONCLUSION AND FUTURE WORK

By using the EG-LDPC codes in the proposed LDPC-VBLAST system, the bit error rate performance can be improved. It is also shown in this thesis that increasing the code rate, along with the error correcting capability of the code, we can maximize the transmission rate due to the increased channel capacity from the multi-transmit and multi-receive antennas system. We have shown the various cases of different code rates and number of antennas in both transmitter and receiver. A lower bound for LDPC-VBLAST system is also provided. The most notable advantage of the proposed LDPC-VBLAST system is the simplicity in the decoding algorithm.

Other types LDPC codes also can be applied. Future improvements can be achieved by implementing the system with different LDPC codes or decoding scheme in order to improve the bit error rate with less complexity, which is the advantage of low density parity check codes. Punctured or extended LDPC codes [4] may be needed in some cases in order to have a certain code length suitable for the given applications. Thus, criteria for designing still needs to be developed.

Interleaving is also expected to improve the proposed system and needs to be evaluated. In [32] the authors show that interleaving and re-decoding in a turbo fashion can improve the performance of multiple antenna systems. Some other publications also show that the application of space-time block codes to multiple antenna systems can result in the reduction of the number of receive antennas in mobile communication applications. However, the channel capacity is then decreased. For wireless applications where the number of antennas is not a constraint, VBLAST with LDPC codes or LDPC-BLAST is a suitable choice.

BIBLIOGRAPHY

[1] C. E. Shannon and W. Weaver, *The Mathematical Theory of Communication,* Urbana, Illinois: University of Illinois Press, 1949.

[2] R. G. Gallager. *Low Density Parity Check Codes*. MIT Press, Cambridge, MA, 1963.

[3] D. J. C. MacKay, "Good error-correcting codes based on very sparse matrices," *IEEE Trans. Inform. Theory*, vol.45, pp. 399-431, Mar 1999.

[4] Y. Kou, S. Lin, and M. P. C. Fossorier, "Low -density parity-check codes based on finite geometries: a rediscovery and new results." *IEEE Trans. Information Theory,* vol47, pp.2711-2736, Nov 2001.

[5] G. J. Foschini and M. J. Gans, "On limits of wireless communication in a fading environment when using multiple antennas," *Wireless Personal Commun.,* vol. 6, no. 3, pp. 311--335, Mar. 1998.

[6] E. Telatar, "Capacity of Multi-Antenna Gaussian Channels," in *Proc. 2001 IEEE Int. Symp. Information Theory*, June 24-29, 2001.

[7] A.Hottinen, O.Tirkkonen, R.Wichman, *Multi-antenna Transceiver Techniques for 3G and Beyond*, UK: Wiley, 2003.

[8] W. Fong, S. Lin, G. Maki, and P. S. Yeh, "Low Density Parity Check Codes: Bandwidth Efficient Channel Coding." in *Proc. of the ESTC2003*, June 24-26, 2003.

[9] D. Sridhara, T. E. Fuja, "Low density parity check codes over groups and rings," in *Proc. of the IEEE Information Theory Workshop 2002,* Oct.20-25, 2002.

[10] Yu Yi, Moon Ho Lee, "Optimized Low-Density Parity-Check (LDPC) code for Bandwidth Efficient Modulation", *in Proc. of the 58th VTC2003*, vol. 4, no. 2, pp. 2367 – 2370, 2003.

[11] S. Lin and D. J. Costello, Jr., *Error Control Coding: Fundamentals and Applications,* Englewood Cliffs, NJ: Prentice-Hall, 1983.

[12] W. W. Peterson and E. J. Weldon, Jr., *Error-Correcting Codes*, 2nd ed., Cambridge, MA: MIT Press, 1972.

[13] T. Kasami, S. Lin, and W.W. Peterson, "Polynomial codes," *IEEE Trans. Inform. Theory*, vol. IT-14, pp. 807–814, Nov. 1968.

[14] M. Fossorier, M. Mihaljevic and H. Imai, "Reduced Complexity Iterative Decoding of Low Density Parity Check Codes Based on Belief Propagation," *IEEE Trans. on Communications*, vol. COM-47, pp. 673-680, May 1999.

[15] T. S. Rappaport, *Wireless Communications: Principles and Practice*, 2nd ed., Upper Saddle River, NJ: Prentice-Hall, 1983.

[16] T. L. Marzetta and B. M. Hochwald, "Capacity of a mobile multiple-antenna communication link in Rayleigh flat fading," *IEEE Trans. Info. Theory*, vol. 45, pp. 139-157, 1999.

[17] W. C. Jakes, *Microwave Mobile Communications*. Piscataway, NJ: IEEE Press, 1994.

[18] Y. R. Zheng and C. Xiao, "Simulation models with correct statistical properties for Rayleigh fading channels," *IEEE Trans. Commun.*, vol. 51, pp. 920–928, June 2003.

[19] C. Xiao, Y. R. Zheng, and N. C. Beaulieu, "Second-order statistical properties of the WSS Jakes' fading channel simulator," *IEEE Trans. Commun.*, vol. 50, pp. 888–891, June 2002.

[20] R. S. Blum, J. H. Winters, "On optimum MIMO with antenna selection," *IEEE International Conference on Communications, 2002,* vol. 1, pp. 386 – 390, April 28-May 2, 2002.

[21] S.L. Ariyavisitakul," Turbo Space-Time Processing to improve wireless Channel Capacity," *IEEE Trans. Commun.*, vol. 48, pp. 1347-1359, August 2000.

[22] X. Li, H. C. Huang, A. Lozano, G. J. Foschini, "Reduced-complexity detection algorithms for systems using multi-element arrays," *Global Telecommunications Conference, 2000. GLOBECOM '00. IEEE* , vol. 2 , pp.1072 – 1076, Nov.27 - Dec.1, 2000 .

[23] P. W. Wolniansky, G. J. Foschini, G. D. Golden, and R. A. Valenzuela, "V-BLAST : An architecture for realizing very high data rates over the rich-scattering wireless channel," *URSI International Symposium on Signals, Systems and Electronics*, pp.295-300, 1998.

[24] A. Ben-Israel, *Generalized inverses: theory and applications.* , Canada: Wiley, 1974.

[25] C. Chen, *Linear system theory and design*, 3rd ed., NY: Oxford University Press, 1998.

[26] L.S. Gradshteyn, I.M. Ryshik, *Table of Integrals series and product*, 6th ed., Academic press, 2000.

[27] J.E. Pečarić, F. Proschan, Y.L. Tong, *Convex functions, partial orderings, and statistical applications*, Mathematics in science and engineering; v.187, CA: Academic Press, 1992.

[28] B.A. Bjerke, J.G. Proakis, "Multiple-antenna diversity techniques for transmission over fading channels," in *Proceedings WCNC'99 Conference,* New Orleans, LA, September 1999.

[29] B. M. Hochwald, *S.T. Brink,* "Achieving near-capacity on a multiple-antenna channel" *IEEE Trans. Commun.* , vol. 51 , pp.389 - 399 , March 2003.

[30] J. G. Proakis, *Digital Communications*, 4th ed. ,NY: McGraw-Hill, 2000.

[31] D. Shiu, G. J. Foschini, M. J. Gans, J. M. Kahn, "Fading Correlation and Its Effect on the Capacity of Multielement Antenna Systems," *IEEE Trans. Commun.*, vol. 48 , pp.502-513.

[32] M. Sellathurai,S. Haykin, " Turbo-BLAST for wireless communications: theory and experiments," *IEEE Trans. on Signal Processing*, vol. 50 , pp. 2538 - 2546 , Oct. 2002

APPENDICES

Appendix A: Derivation of $\det\left(I_{N_r} + \frac{\rho}{N_t}\mathbf{H}\mathbf{H}^H\right)$ and $\det\left(I_{N_t} + \frac{\rho}{N_t}\mathbf{H}^H\mathbf{H}\right)$

Let $\mathbf{H}$ be an $N_r \times N_t$ matrix, and $\frac{\rho}{N_t}\mathbf{H}^H$ is $N_t \times N_r$ matrix. Define the partitioned matrices $\mathbf{N}$, $\mathbf{Q}$ and $\mathbf{P}$ as

$$\mathbf{N} = \begin{bmatrix} \mathbf{I}_{N_r} & \mathbf{H} \\ \mathbf{0} & \mathbf{I}_{N_t} \end{bmatrix}, \mathbf{Q} = \begin{bmatrix} \mathbf{I}_{N_r} & \mathbf{0} \\ -\frac{\rho}{N_t}\mathbf{H}^H & \mathbf{I}_{N_t} \end{bmatrix}, \mathbf{P} = \begin{bmatrix} \mathbf{I}_{N_r} & -\mathbf{H} \\ \frac{\rho}{N_t}\mathbf{H}^H & \mathbf{I}_{N_t} \end{bmatrix}.$$

Then,

$$\mathbf{NP} = \begin{bmatrix} \mathbf{I}_{N_r} + \frac{\rho}{N_t}\mathbf{H}\mathbf{H}^H & -\mathbf{H} + \mathbf{H} \\ \frac{\rho}{N_t}\mathbf{H}^H & \mathbf{I}_{N_t} \end{bmatrix} = \begin{bmatrix} \mathbf{I}_{N_r} + \frac{\rho}{N_t}\mathbf{H}\mathbf{H}^H & \mathbf{0} \\ \frac{\rho}{N_t}\mathbf{H}^H & \mathbf{I}_{N_t} \end{bmatrix}$$

$$\mathbf{QP} = \begin{bmatrix} \mathbf{I}_{N_r} & -\mathbf{H} \\ -\frac{\rho}{N_t}\mathbf{H}^H + \frac{\rho}{N_t}\mathbf{H}^H & \frac{\rho}{N_t}\mathbf{H}^H\mathbf{H} + \mathbf{I}_{N_t} \end{bmatrix} = \begin{bmatrix} \mathbf{I}_{N_r} & -\mathbf{H} \\ \mathbf{0} & \frac{\rho}{N_t}\mathbf{H}^H\mathbf{H} + \mathbf{I}_{N_t} \end{bmatrix}.$$

Since **NP** and **QP** are block triangular matrices, the determinants of **NP** and **QP** can be obtained by multiplication of the diagonal block determinants. Thus,

$$\det(\mathbf{NP}) = \det(\mathbf{I}_{N_r} + \tfrac{\rho}{N_t}\mathbf{H}\mathbf{H}^H) * \det(\mathbf{I}_{N_t})$$

$$\det(\mathbf{QP}) = \det(\mathbf{I}_{N_r}) * \det(\tfrac{\rho}{N_t}\mathbf{H}^H\mathbf{H} + \mathbf{I}_{N_t}).$$

But

$$\det(\mathbf{NP}) = \det(\mathbf{N})\det(\mathbf{P}) = \det(\mathbf{P})$$

$$\det(\mathbf{QP}) = \det(\mathbf{Q})\det(\mathbf{P}) = \det(\mathbf{P}).$$

Therefore,

$$\det(\mathbf{NP}) = \det(\mathbf{QP})$$

$$\det(\mathbf{I}_{N_r} + \tfrac{\rho}{N_t}\mathbf{H}\mathbf{H}^H) * \det(\mathbf{I}_{N_t}) = \det(\mathbf{I}_{N_r}) * \det(\tfrac{\rho}{N_t}\mathbf{H}^H\mathbf{H} + \mathbf{I}_{N_t})$$

$$\det(\mathbf{I}_{N_r} + \tfrac{\rho}{N_t}\mathbf{H}\mathbf{H}^H) = \det(\mathbf{I}_{N_t} + \tfrac{\rho}{N_t}\mathbf{H}^H\mathbf{H}). \qquad \text{(A1)}$$

The above determinant can also be calculated from its eigenvalues. In practice, it is reasonable to assume that $\mathbf{H}$ has full column rank when $N_r \geq N_t$, and full row rank when $N_r \leq N_t$, i.e., rank=$(\min\{N_t, N_r\})$. Then, $\mathbf{H}^H\mathbf{H}$, with rank N_t, has N_t eigenvalues. $\mathbf{H}\mathbf{H}^H$, with rank N_r, has N_r eigenvalues. It has been shown in [25] that $\mathbf{H}^H\mathbf{H}$ or $\mathbf{H}\mathbf{H}^H$ are symmetric, real, and positive definite matrices, have the same nonzero eigenvalues but may have different numbers of zero eigenvalues. It will be seen later that the determinant depends only on the nonzero eigenvalues, which, therefore, are atmost $\min\{N_t, N_r\}$.

In the case of the VBLAST system where $N_r \geq N_t$, we choose the matrix $\mathbf{H}^H\mathbf{H}$. Using a similarity transformation, $\mathbf{H}^H\mathbf{H}$ can be decomposed into

$$\mathbf{H}^H\mathbf{H} = \mathbf{Q}\mathbf{D}\mathbf{Q}^{-1}, \tag{A2}$$

where $\mathbf{Q}$ is an $N_t \times N_t$ orthogonal matrix. $\mathbf{D}$ is a diagonal matrix with its diagonal entries are equal to the eigenvalues λ of $\mathbf{H}^H\mathbf{H}$. Then,

$$\begin{aligned}
\det(\mathbf{I}_{N_t} + \tfrac{\rho}{N_t}\mathbf{H}^H\mathbf{H}) &= \det(\mathbf{Q}\mathbf{Q}^{-1} + \tfrac{\rho}{N_t}\mathbf{Q}\mathbf{D}\mathbf{Q}^{-1}) \\
&= \det(\mathbf{Q}(\mathbf{I}_{N_t} + \tfrac{\rho}{N_t}\mathbf{D})\mathbf{Q}^{-1}) \\
&= \det(\mathbf{Q})\det\,(\mathbf{I}_{N_t} + \tfrac{\rho}{N_t}\mathbf{D})\,\det(\mathbf{Q}^{-1}) \\
&= \det(\mathbf{I}_{N_t})\det\,(\mathbf{I}_{N_t} + \tfrac{\rho}{N_t}\mathbf{D}) \\
&= \det\,(\mathbf{I}_{N_t} + \tfrac{\rho}{N_t}\mathbf{D}) \\
&= \prod_{i=1}^{N_t}(1 + \tfrac{\rho}{N_t}\lambda_i).
\end{aligned} \tag{A3}$$

Without loss of generality, for either $\det(\mathbf{I}_{N_t} + \frac{\rho}{N_t}\mathbf{H}^H\mathbf{H})$ or $\det(\mathbf{I}_{N_r} + \frac{\rho}{N_t}\mathbf{H}\mathbf{H}^H)$ we can write

$$\prod_{i=1}^{N_t}(1+\frac{\rho}{N_t}\lambda_i) \rightarrow \prod_{i=1}^{\min(N_t,N_r)}(1+\frac{\rho}{N_t}\lambda_i).$$

Therefore, the logarithm of determinant in equation (A1) is equal to

$$\log_2\left[\det\left(I_{N_r}+\frac{\rho}{N_t}\mathbf{H}\mathbf{H}^H\right)\right]=\sum_{i=1}^{\min(N_t,N_r)}\log_2\left[(1+\frac{\rho}{N_t}\lambda_i)\right]. \quad \text{(A4)}$$

Appendix B: Jensen's inequality application in convex, and concave function

This section explains the convex and concave function. We also provide the details of the convexity in Jensen's sense and its application which [6] and [7] use in the derivation of equation (29). In fact, equation (29) uses the property of concave function which is the reverse property of convex function [27]. Therefore, the following details are the information of convex function and its property. Later we will apply the reverse property to the concave function.

In [27] provide the definition of a convex function is provided. $f(x)$ is convex on an interval [a, b] $\rightarrow \Re$ if for all x_1, x_2

$$f(\alpha x_1+(1-\alpha)x_2)\leq \alpha f(x_1)+(1-\alpha)f(x_2) \quad \text{(B1)}$$

where $\alpha \in [0,1]$ and x_1, x_2 is any value on an interval [a, b]. For a concave function, the inequality of the property above is reversed for all $\alpha \in [0,1]$ and x_1, x_2 on an interval [a, b].

The above definition is also the similar to the definition provided by Jensen in 1905 who defined a convex function using inequalities. A function $f(x)$ is called *convex in the Jensen sense*, or *J-convex* , on interval interval [a, b] $\rightarrow \Re$ if for all x_1, x_2

$$f(\frac{x_1+x_2}{2}) \le \frac{f(x_1)+f(x_2)}{2} \tag{B2}$$

where x_1, x_2 lie on an interval [a, b]. It is remarked in [27] that Jensen's original paper mentioned that (B2) was also proved by Hölder in 1889, assuming that $f(x)$ is twice differentiable on [a, b], then $f''(x) \ge 0$ on the interval.

If $f(x_i)$ is convex on interval $x_i \in [a,b] \rightarrow \Re, i = 1,...,n$ $(n \ge 2)$, then the general form of Jensen's inequality can be written

$$f\left(\frac{1}{P_n}\sum_{i=1}^{n} p_i x_i\right) \le \frac{1}{P_n}\sum_{i=1}^{n} p_i f(x_i) \tag{B3}$$

where $p_i > 0$, $i = 1,...,n$ $(n \ge 2)$ and $P_n = \sum_{i=1}^{n} p_i$. In the case $p_1 = p_2 = ... = p_n$ then

$$f\left(\frac{1}{n}\sum_{i=1}^{n} x_i\right) \le \frac{1}{n}\sum_{i=1}^{n} f(x_i). \tag{B4}$$

This inequality is also applied in probability and statistic. When x_i becomes a random variable X_i, [27] provides a Jensen's inequality theorem as follow.

For $n \ge 1$, let $\mathbf{X} = (X_1,...,X_n)$ be an n-dimensional random variable and $F(\mathbf{x}) = P[\mathbf{X} \le \mathbf{x}]$ is the cumulative distribution function of $\mathbf{X}$. A continuos convex function $\phi : A \rightarrow \Re$ where $A \subset \Re^n$ is an open convex set such that $P[\mathbf{X} \in A]$=1 then

$$E\{\phi(\mathbf{X})\} = \int_A \phi(x) dF(\mathbf{x}) \ge \phi(\boldsymbol{\mu}) \tag{B5}$$

where $\boldsymbol{\mu} = (E\{X_1\},...,E\{X_n\})$ and $\boldsymbol{\mu} \in A$.

The opposite to convex function, $g(x)$ is a concave function over an interval [a,b] if $-g(x)$ is a convex function. Therefore

$$g(\frac{x_1+x_2}{2}) \geq \frac{g(x_1)+g(x_2)}{2} \tag{B6}$$

for any two points x_1, x_2 on an interval [a, b] $\rightarrow \Re$. Its second derivative is then $g''(x) < 0$ for all x on the interval. The inequality in (B3), (B4), (B5) for concave function $g(x)$ is also reverse to

$$g\left(\frac{1}{P_n}\sum_{i=1}^{n} p_i x_i\right) \geq \frac{1}{P_n}\sum_{i=1}^{n} p_i g(x_i) \tag{B7}$$

$$g\left(\frac{1}{n}\sum_{i=1}^{n} x_i\right) \geq \frac{1}{n}\sum_{i=1}^{n} g(x_i) \tag{B8}$$

$$E\{\phi(\mathbf{X})\} = \int_A \phi(x) dF(\mathbf{x}) \leq \phi(\boldsymbol{\mu}). \tag{B9}$$

Finally, since the logarithm function is used in equation (29). We show that $\log_b x$ is concave function as follow:

$$\begin{aligned} \frac{d^2}{dx^2}(g(x)) &= \frac{d^2}{dx^2}(\log_b x) \\ &= -\frac{1}{x^2 \ln b} \end{aligned}$$

Since $\ln b$ are always positive, then $\frac{d^2}{dx^2}(\log_b x) < 0$ for all x. Therefore, it is a concave function.